Post-print of: Kulkowski K., Grochowski M., Duzinkiewicz K., Kobylarz A.: Nuclear Power Plant Steam Turbine - Modeling for Model Based Control Purposes. APPLIED MATHEMATICAL MODELLING. Vol. 48, (2017), p. 491-515.
DOI: 10.1016/j.apm.2017.04.008

Nuclear power plant steam turbine—Modeling for model based control purposes

Karol Kulkowski Michał Grochowski, Kazimierz Duzinkiewicz, Anna Kobylarz

Gdansk University of Technology, Faculty of Electrical and Control Engineering, G. Narutowicza 11/12, Gdansk 80-233, Poland

abstract

The nature of the processes taking place in a nuclear power plant (NPP) steam turbine is the reason why their modeling is very difficult, especially when the model is intended to be used for on-line optimal model based process control over a wide range of oper- ating conditions, caused by changing electrical power demand e.g. when combined heat and power mode of work is utilized. The paper presents three nonlinear models of NPP steam turbine, which are: the static model, and two dynamic versions, detailed and sim- plified. As the input variables, the models use the valve opening degree and the steam flow properties: mass flow rate, pressure and temperature. The models enable to get ac- cess to many internal variables describing process within the turbine. They can be treated as the output or state variables. In order to verify and validate the models, data from the WWER-440/213 reactor and the 4 CK 465 turbine were utilized as the benchmark. The per- formed simulations have shown good accordance of the static and dynamic models with the benchmark data in steady state conditions. The dynamic models also demonstrated good behavior in transient conditions. The models were analyzed in terms of computa- tional load and accuracy over a wide range of varying inputs and for different numerical calculation parameters, especially time step values. It was found that the detailed dynamic model, due to its complexity and the resultant long calculation time, is not applicable in advanced control methods, e.g. model predictive control. However, the introduced simplifi- cations significantly decreased the computational load, which enables to use the simplified model for on-line control.

Keywords: Nuclear power plant, Steam turbine, Modeling, Models for control

1. Introduction

Nowadays, the requirements of energy markets often force nuclear power plants (NPPs) to work at an operating point which differs from the nominal value and varies in time. Moreover, a very common opinion is, that in the near future co-generated NPPs (combined heat and electricity generation in a NPP) would be designed in order to increase the energetic efficiency [1–3]. A combined heat and power (CHP) NPP needs to work in varying regimes, and the commonly used control methods based on PID controllers and operation rules are not sufficiently robust and resilient to handle this mode of operation efficiently and effectively. More advanced control methods require employing corresponding process models. The paper focuses on models of NPP steam turbines and their applicability for control purposes. The steam turbines are most

http://dx.doi.org/10.1016/j.apm.2017.04.008

Acronyms

NPP	nuclear power plant
CHP	combined heat and power
SISO	single-input-single-output
PID	proportional-integral-derivative
MPC	model predictive control
CV	control valve
ST	steam turbine
HP	high pressure
LP	low pressure
DS	dead space
MS	moisture separator
R	reheater

Abbreviations

i, *o*	input, output
in, out	inlet, outlet
nom	nominal
H	adiabatic exponent
W	water
S	steam
V	accumulation volume
v	specific volume
avg	average

Notation

M, *P*, *T*	mass flow rate, pressure, temperature
h, Δh	theoretical enthalpy, theoretical enthalpy drop
N	power
CV	index of control valve
DS	index of the dead space
i_{vent}	index of *i*th stage with vent
$s \in \{\text{HP,LP}\}$	index of the steam turbine section
$n_s, i \in \{1,\ldots,n_s\}$	number of stages in *s*th section of the steam turbine, index of stage
$m_s, j \in \{1,\ldots,m_s\}$	number of groups in *s*th section of the steam turbine, index of the group
R	index of the reheater
MS	index of the moisture separator
X	vapor fraction
η	efficiency
τ	time constant

important elements of power generation systems. However, not many models are available in practice, which could be used for advanced control and monitoring purposes. Models proposed in many published papers are linear or linearized around one nominal working point and not appropriate in the considered case as they are often based on iterative solving methods. In the paper nonlinear steam turbine models, static and dynamic have been proposed, and their applicability to control system design has been analyzed.

The steam turbine itself consists of stages with blades. The basic principle which describes energy conversion from thermal to mechanical energy is the Rankine cycle. If the design process makes it necessary, the steam can be reheated between turbine parts without pressure change. Additionally, in order to improve the steam properties, a moisture separator can be applied.

The inputs of the static model are the steam flow properties such as: mass flow rate, pressure, and temperature. The outputs of the model are: mass flow rates, pressures, temperatures and theoretical power, all calculated for each defined stage. The model behavior was validated based on data from the nuclear reactor WWER-440/213, the 4 CK 465 turbine sets, and the electric power generator GTHW-600 that were going to be built in Żarnowiec in Poland in the 20th century [4,5].

The control structures for steam turbines are commonly designed as SISO systems, based on and limited to basic controllers such as PID controllers, that are valid only at a specified (steady state) operating point. However, most advanced control methods that enable optimized control, such as MPC [6], require dynamic models, which describe the processes taking place in the steam turbine with sufficient accuracy [7] and offer economically efficient and improved control accuracy (comparing with the aforementioned basic control methods) over a wide range of operating conditions. Hence, the dynamic nonlinear models of the steam turbine are analyzed.

Described models enable appliance of advanced control methods, taking into account occurring dynamic processes, according to the requirements expressed in [8–11]. The models used in [8,9] are lumped parameters models, also referred to as the point dynamic models. The same approach is used in the here presented models, assuming that the steam influence on the turbine blades in different directions is neglected.

The model enables to calculate process output variables individually in each stage, which leads to high computational complexity and the resultant high demands concerning computer hardware parameters. In order to speed up the calculation process, certain model simplifications were introduced.

The models presented in the paper return the response as functions of the input variable scenarios, having the form of the steam flow properties before the control valve and the valve opening degree given as trajectories over time. A similar approach was used in [7] where model implemented in ATHLET® code takes mass flow and enthalpy of the steam on the input of turbine stage in order to calculate the pressure at the output of the stage. In [12,13] authors present mathematical model using known input–output relations of the system components. The solution utilizes iterative method of gaining the variables (they are updated until convergent values are obtained). Steam turbine can be modeled using lumped parameters like it was applied in this paper and in [14]. Unlike iterative methods, presented approach does not require calculating the variables, with an optional correction described in [15]. Moreover, the here presented models allow to analyze the steam turbine processes stage by stage [16]. In case of models presented in this paper, it is possible to use them as the input–output models for the control purposes e.g. using pressure, temperature and mass flow rate as inputs and total power as output as in [17]. Moreover, they enable gaining access to variables inside turbine sections what could be useful in case of water extractions control e.g. in case of heat and power cogeneration. What is more, one of the simplifications applied and presented in this paper concerns modeling based on merging stages into groups. Similar approach can be also observed in other papers, like in [4,18].

The paper is organized as follows: Section 2 presents the objectives and scopes of the paper, then Section 3 describes steam turbine models with theoretical fundamentals of steam turbine modeling. Further, in Section 4 presented models are confronted with the reference data and each other. Finally, Section 5 concludes the paper and presents on-going and future authors research at this field.

2. Scope and objectives

The objective of the paper is to propose nuclear power plant steam turbine models for control purposes and to compare their suitability for on-line model-based control over a wide range of turbine operating conditions.

The static and dynamic turbine models were designed and implemented in Matlab®/Simulink® (version 2015a). The steam turbine considered as a system was divided into several subsystems. These are: control valve, dead space, turbine stages grouped into two parts, moisture separator and reheater. For each subsystem input and output variables were defined and model structure was presented. The 4 CK 465 turbine of the WWER-440 reactor, which was planned to be built in Żarnowiec in Poland in the 20th century was used as the benchmark. The models were verified on the data from [19]. As the model intended to be applied in real time system, time of the computation with the model should be constrained from above by an appropriate maximal values. Time of the computation with the model depends mainly on the time step of calculation. Greater the time step of calculation—smaller the time of the computation with the model. On the other hand, from numerical stability conditions the time step of calculation cannot be too large. The models were initially analyzed to assess the numerical calculation parameters, mainly time step values. Based on this analysis, the maximal time step was established which provides calculation stability.

Next, the dynamic model was simplified in order to decrease the computational load. The main model modifications included: merging stages into groups, linear approximation of the process variable values calculated after the reheater, approximating steam separator values, averaging parameters, assuming time constants as independent in respect of the changing load.

All models were compared using the same testing scenario in order to show their behavior over a wide range of varying inputs. The introduced model modifications significantly decreased the calculation time, at the same time maintaining an acceptable accuracy of the computation with the model. What is more, the simplifications allowed to meet the real time requirements.

Finally, the conclusions about the suitability of the models for on-line control purposes were formulated.

3. Steam turbine models

Each steam turbine model presented in the paper is the input–output model. The modeled turbine is a two-part steam turbine designed for nuclear power plant with a steam reheater and a moisture separator between each part. The demonstration scheme of the turbine is the same for each model and includes main turbine parts, such as: inlet valve, high pressure part, low pressure part, moisture separator, and reheater. The full scheme of the turbine is shown in Fig. 1. Models were built with the general intention to apply them in the control system design. The process, which makes the basis for modeling is the steam expansion along the whole turbine. The modeling is based inter alia on the Stodola–Flügel cone law and

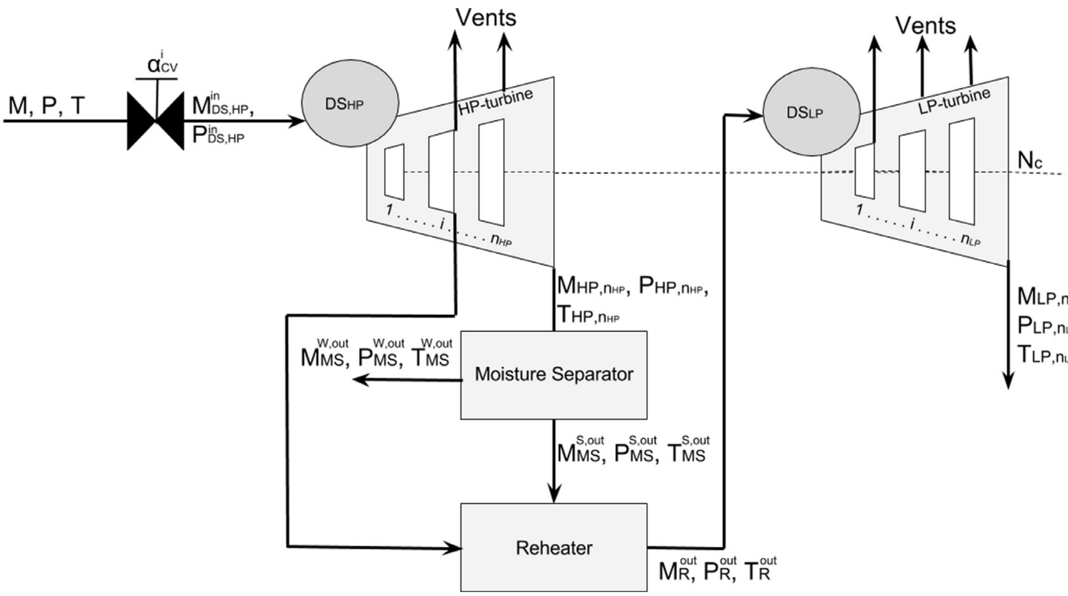

Fig. 1. Scheme of the modeled steam turbine with moisture separator and interstage steam superheating.

the steam properties with values given in the tables. Each model was built as a composition of sub models of recognizable parts of the steam turbine system. Parameters of developed models are shown in Table A.1 in the Appendix.

3.1. Static model

The model consists of sub models of devices such as: reheater, moisture separator, stages with and without vents, and accumulation spaces referred to as dead spaces (DS). All sub models are described by such variables as: mass flow rate *M*, pressure *P*, temperature *T*, and additional variables characterizing a given sub model. Many relations base on the values defined for the nominal point of steam turbine operation, briefly referred to as the nominal values. The nominal point is understood here as the state of steam turbine operation when it works in its full power under 100% load. Additionally, below equations describing presented sub-models. Appearing parameters were named and described.

3.1.1. Control valve

The control valve is a commonly used actuator of turbine power control system. The behavior of this element of the turbine system is characterized by values of the mass flow, pressure of the working medium at the inlet and outlet of the element. At the steady state condition the current opening degree $\propto_{CV}^{0}$ is equal to the reference opening degree $\propto_{\mathrm{CV}}^{i}$ (1). The pressure $P_{\mathrm{CV}}^{\mathrm{out}}$ (2) at the outlet of the element and output mass flow rate $M_{\mathrm{CV}}^{\mathrm{out}}$ (3) are proportional to the product of their nominal values, the ratio of current valve opening degree $\propto_{\mathrm{CV}}^{0}$ and its nominal value $\propto_{\mathrm{CV}}^{\mathrm{nom}\ 0}$ and in case of output mass flow rate with additional product of the ratio of input pressure P and its nominal value P^{nom} (3). To achieve more accurate results in transient states output mass flow rate of control valve can be also calculated using formula (4). In case of the static model relation given in Eq. (3) is sufficient.

$$\propto_{\mathrm{CV}}^{0} = \propto_{\mathrm{CV}}^{i}, \tag{1}$$

$$P_{\mathrm{CV}}^{\mathrm{in}} = P;$$
$$P_{\mathrm{CV}}^{\mathrm{out}} = P_{\mathrm{CV}}^{\mathrm{nom,\ out}} \frac{\propto_{\mathrm{CV}}^{0}}{\propto_{\mathrm{CV}}^{\mathrm{nom}\ 0}}, \tag{2}$$

$$M_{\mathrm{CV}}^{\mathrm{in}} = M;$$
$$M_{\mathrm{CV}}^{\mathrm{out}} = M_{\mathrm{CV}}^{\mathrm{nom,\ out}} \frac{P}{P^{\mathrm{nom}}} \frac{\propto_{CV}^{0}}{\propto_{\mathrm{CV}}^{\mathrm{nom}\ 0}}, \tag{3}$$

$$M_{\mathrm{CV}}^{\mathrm{out}} = M_{\mathrm{CV}}^{\mathrm{nom,out}} \left(\frac{A_{\mathrm{CV}} \left(\frac{\propto_{\mathrm{CV}}^{0}}{\propto_{\mathrm{CV}}^{\mathrm{nom}\ 0}} \right)^{\frac{H_{\mathrm{CV}}-1}{H_{\mathrm{CV}}}}}{\sqrt{1 - B_{\mathrm{CV}} \left(\frac{\propto_{\mathrm{CV}}^{0}}{\propto_{\mathrm{CV}}^{\mathrm{nom}\ 0}} \right)^{\frac{H_{\mathrm{CV}}-1}{H_{\mathrm{CV}}}}}} \sqrt{\left(\frac{P_{\mathrm{CV}}^{\mathrm{out}}}{P_{\mathrm{CV}}^{\mathrm{in}}} \right)^{\frac{2}{H_{\mathrm{CV}}}} - \left(\frac{P_{\mathrm{CV}}^{\mathrm{out}}}{P_{\mathrm{CV}}^{\mathrm{in}}} \right)^{\frac{H_{\mathrm{CV}}-1}{H_{\mathrm{CV}}}}} \right), \tag{4}$$

where P^{nom} is nominal pressure of the live steam, $P_{\mathrm{CV}}^{\mathrm{nom,out}}$ is nominal steam pressure at CV outlet, $\propto_{\mathrm{CV}}^{\mathrm{nom}\ 0}$ is nominal valve opening degree, $M_{\mathrm{CV}}^{\mathrm{nom,out}}$ is nominal control valve output mass flow rate, H_{CV} is control valve adiabatic exponent, A_{CV}, B_{CV} are valve mass flow rate coefficients.

3.1.2. Dead space

The so-called dead spaces, which are the accumulation spaces between specified parts of the presented model, are characterized by pressure and temperature drops. The lack of leak was assumed, so all inlet mass flow is to pass through the dead spaces to the outlet (5). Assumptions from [5] were adopted that the pressures at the outlet and the inlet are roughly in a linear relationship with a coefficient of proportionality equal to the ratio of the nominal pressures (6). The temperature at the outlet of the dead space is approximated by the function of the outlet pressure, based on the data received from producer (7). The dead space sub model is described in Eqs. (5)–(7) presented below:

$$\begin{aligned} &M_{\mathrm{DS},s}^{\mathrm{in}} = M_{\mathrm{CV}}^{\mathrm{out}} && \text{for } s = \mathrm{HP}; \\ &M_{\mathrm{DS},s}^{\mathrm{in}} = M_{R}^{\mathrm{out}} && \text{for } s = \mathrm{LP}; \\ &M_{\mathrm{DS},s}^{\mathrm{out}} = M_{\mathrm{DS},s}^{\mathrm{in}}, && \text{for } s \in \{\mathrm{HP}, \mathrm{LP}\}, \end{aligned} \tag{5}$$

$$\begin{aligned} &P_{\mathrm{DS},s}^{\mathrm{in}} = P_{\mathrm{CV}}^{\mathrm{out}} && \text{for } s = \mathrm{HP}; \\ &P_{\mathrm{DS},s}^{\mathrm{in}} = P_{R}^{\mathrm{out}} && \text{for } s = \mathrm{LP}; \\ &P_{\mathrm{DS},s}^{\mathrm{out}} = \frac{P_{\mathrm{DS},s}^{\mathrm{in}}}{P_{\mathrm{DS},s}^{\mathrm{nom,in}}} P_{\mathrm{DS},s}^{\mathrm{nom,out}} && \text{for } s \in \{\mathrm{HP}, \mathrm{LP}\}, \end{aligned} \tag{6}$$

$$T_{\mathrm{DS},s}^{\mathrm{out}} = A_{\mathrm{DS}} P_{\mathrm{DS},s}^{\mathrm{out}^{B_{\mathrm{DS}}} P_{\mathrm{DS},s}^{\mathrm{out}\ C_{\mathrm{DS}}}} \quad \text{for } s \in \{\mathrm{HP}, \mathrm{LP}\} \tag{7}$$

where $P_{\mathrm{DS},s}^{\mathrm{nom,in}}$, $P_{\mathrm{DS},s}^{\mathrm{nom,out}}$ are nominal inlet and outlet dead space pressures and $T_{\mathrm{DS},s}^{\mathrm{in}}$, $T_{\mathrm{DS},s}^{\mathrm{nom,out}}$ are nominal inlet and outlet dead space temperatures, A_{DS}, B_{DS}, C_{DS} are temperature coefficients of the dead space.

3.1.3. Stages

The mass flow rate at the outlet of the stage without vents is described in Eq. (8) based on the Stodola–Flügel cone law, and in Eq. (9) in stages with vents, assuming proportional steam distribution into the next stage and into the vent. The pressure is given in Eq. (10), adopting the same assumptions as for the dead space. Temperature of the steam calculated along the steam turbine from its inlet can be described and calculated using the same structure of formula (11) with slightly different function coefficients dependent on the stage properties and obtained in process of approximation. In case of two last stages of the steam turbine, because of their character mainly caused by their location (they are placed near the condenser), the structure of function approximating temperature in these stages differs from the rest of the stages—Eqs. (12) and (13). Along each stage a drop of enthalpy caused by the process of steam expansion occurs. Formula describing the enthalpy drop Δh approximated based on the factory data and the steam properties obtained from the tables is presented in Eq. (14).

$$M_{s,i}^{\mathrm{out}} = \sqrt{\frac{T_{s,i}^{\mathrm{nom,in}}}{T_{s,i}^{\mathrm{in}}} \frac{\left(P_{s,i}^{\mathrm{in}}\right)^2 - \left(P_{s,i}^{\mathrm{out}}\right)^2}{\left(P_{s,i}^{\mathrm{nom,in}}\right)^2 - \left(P_{s,i}^{\mathrm{nom,out}}\right)^2}} M_{s,i}^{\mathrm{nom,out}} \qquad \text{for } s \in \{\mathrm{HP}, \mathrm{LP}\}, i \in \{1, \ldots, n_s\}, \tag{8}$$

$$M_{s,i_{\mathrm{vent}}}^{\mathrm{out}} = \frac{M_{s,i=i_{\mathrm{vent}}}^{\mathrm{out}}}{M_{s,i=i_{\mathrm{vent}}}^{\mathrm{nom,out}}} M_{s,i_{\mathrm{vent}}}^{\mathrm{nom,out}} \qquad \text{for } s \in \{\mathrm{HP}, \mathrm{LP}\}, i_{\mathrm{vent}} \in \{ i_{\mathrm{vent},1}, \ldots, n_{\mathrm{vent},s}\}, \tag{9}$$

$$\begin{aligned} &P_{s,i}^{\mathrm{in}} = P_{\mathrm{DS},s}^{\mathrm{out}} && \text{for } i = 1, s \in \{\mathrm{HP}, \mathrm{LP}\}; \\ &P_{s,i}^{\mathrm{in}} = P_{s,i-1}^{\mathrm{out}} && \text{for } i \in \{2, \ldots, n_s\}; \\ &P_{s,i}^{\mathrm{out}} = \frac{P_{s,i}^{\mathrm{in}}}{P_{s,i}^{\mathrm{nom,in}}} P_{s,i}^{\mathrm{nom,out}} && \text{for } s \in \{\mathrm{HP}, \mathrm{LP}\}, \ i \in \{1, \ldots, n_s\}, \end{aligned} \tag{10}$$

$$T_{s,i}^{\mathrm{out}} = A_T \left(P_{s,i}^{\mathrm{out}}\right)^{B_T \left(P_{s,i}^{\mathrm{out}}\right)^{C_T}} \qquad \text{for } s \in \{\mathrm{HP}, \mathrm{LP}\}, \ i \in \{1, \ldots, n_{\mathrm{HP}}\} \wedge \in \{1, \ldots, n_{\mathrm{LP}} - 2\}, \tag{11}$$

$$T_{\mathrm{LP},k-1}^{\mathrm{out}} = D_T + E_T \frac{P_{\mathrm{LP},n_{\mathrm{LP}}-2}^{\mathrm{in}}}{P_{\mathrm{LP},n_{\mathrm{LP}}-2}^{\mathrm{nom,in}}} T_{\mathrm{LP},n_{\mathrm{LP}}-1}^{\mathrm{nom,out}}, \tag{12}$$

$$T_{\mathrm{LP},k}^{\mathrm{out}} = F_T + G_T \frac{P_{\mathrm{LP},n_{\mathrm{LP}}-1}^{\mathrm{in}}}{P_{\mathrm{LP},n_{\mathrm{LP}}-1}^{\mathrm{nom,in}}} T_{\mathrm{LP},n_{\mathrm{LP}}}^{\mathrm{nom,out}}, \tag{13}$$

$$\Delta h_{s,i}^{\text{out}} = \Delta h_{s,i}^{\text{nom,out}} \left(\frac{T_{s,i}^{\text{in}}}{T_{s,i}^{\text{nom,in}}} \frac{1 - \left(\frac{P_{s,i}^{\text{out}}}{P_{s,i}^{\text{in}}}\right)^{\frac{H_{s,i}-1}{H_{s,i}}}}{1 - \left(\frac{P_{s,i}^{\text{nom,out}}}{P_{s,i}^{\text{nom,in}}}\right)^{\frac{H_{s,i}-1}{H_{s,i}}}} \right) \quad \text{for } s \in \{\text{HP}, \text{LP}\}, i \in \{1, \ldots, n_s\}. \tag{14}$$

In these formulas: $M_{s,i}^{\text{nom,out}}$—nominal output mass flow rate of the ith turbine stage; $P_{s,i}^{\text{nom,in}}$—nominal input pressure of the ith turbine stage; $P_{s,i}^{\text{nom,out}}$—nominal output pressure of the ith turbine stage; $T_{s,i}^{\text{nom,in}}$—nominal input temperature of the ith turbine stage; $M_{\text{Vent},s,i}^{\text{nom,out}}$—nominal mass flow rate of the vent on the outlet of the ith stage; A_T, B_T, C_T, D_T, E_T, F_T, G_T,—temperature coefficients, obtained from the factory data; $\Delta h_{s,i}^{\text{nom,out}}$—nominal enthalpy drop in the ith stage; $T_{s,i}^{\text{nom,in}}$—nominal inlet temperature of the ith stage; $H_{s,i}$—adiabatic exponent of the ith stage; $P_{s,i}^{\text{nom,out}}$—nominal output pressure of the ith stage; $P_{s,i}^{\text{nom,in}}$—nominal inlet pressure of the ith stage.

3.1.4. Moisture separator

The moisture separator extracts the moisture from the steam. Based on the experts' knowledge this process is modeled by linear relations described by Eqs. (15) and (16). These relations enable to calculate the steam mass flow rate $M_{\text{MS}}^{S,\text{out}}$ at the moisture separator outlet and the mass flow rate of the extracted water $M_{\text{MS}}^{W,\text{out}}$ at the moisture separator outlet based on the outlet mass flow rate $M_{\text{HP},n_{\text{HP}}}^{\text{out}}$ of the high pressure section. The mass flow rate and the temperature of water can be also calculated alternatively using approximation based on factory data given from the producer Eqs. (16) and (17). The steam pressure $P_{\text{MS}}^{S,\text{out}}$ and the water pressure $P_{\text{MS}}^{W,\text{out}}$ at the outlet of moisture separator are equal to the output pressure of HP section pressure $P_{\text{HP},n_{\text{HP}}}^{\text{out}}$ see Eqs. (19) and (20). Analogically, the steam $T_{\text{MS}}^{S,\text{out}}$ and the water temperature $T_{\text{MS}}^{W,\text{out}}$ at the outlet of moisture separator are equal to the temperature on the outlet of HP section $T_{\text{HP},n_{\text{HP}}}^{\text{out}}$ see Eqs. (21) and (22) and analogically Eq. (18).

$$\begin{aligned} M_{\text{MS}}^{S,\text{in}} &= M_{\text{HP},n_{\text{HP}}}^{\text{out}}; \\ M_{\text{MS}}^{S,\text{out}} &= \tfrac{x^{\text{in}}}{x^{\text{out}}} M_{\text{MS}}^{S,\text{in}}, \end{aligned} \tag{15}$$

$$M_{\text{MS}}^{W,\text{out}} = \left(1 - \frac{x^{\text{in}}}{x^{\text{out}}}\right) M_{\text{MS}}^{S,\text{in}}, \tag{16}$$

$$M_{\text{MS}}^{W,\text{out}} = M_{\text{MS}}^{\text{nom},W,\text{out}} \left(P_{T1} \frac{M_{\text{MS}}^{S,\text{in}}}{M_{\text{MS}}^{\text{nom},S,\text{in}}} - P_{T2} \frac{M_R^{\text{out}}}{M_R^{\text{nom,out}}} \right), \tag{17}$$

$$\begin{aligned} T_{\text{MS}}^{W,\text{in}} &= T_{\text{HP},n_{\text{HP}}}^{\text{out}}; \\ T_{\text{MS}}^{W,\text{out}} &= T_{\text{MS}}^{\text{nom},W,\text{out}} \left(P_{T3} \tfrac{T_{\text{MS}}^{W,\text{in}}}{T_{\text{MS}}^{\text{nom},W,\text{in}}} + P_{T4} \right), \end{aligned} \tag{18}$$

$$\begin{aligned} P_{\text{MS}}^{S,\text{in}} &= P_{\text{HP},n_{\text{HP}}}^{\text{out}}; \\ P_{\text{MS}}^{S,\text{out}} &= P_{\text{MS}}^{S,\text{in}}, \end{aligned} \tag{19}$$

$$\begin{aligned} P_{\text{MS}}^{W,\text{in}} &= P_{\text{HP},n_{\text{HP}}}^{\text{out}}; \\ P_{\text{MS}}^{W,\text{out}} &= P_{\text{MS}}^{W,\text{in}}, \end{aligned} \tag{20}$$

$$\begin{aligned} T_{\text{MS}}^{S,\text{in}} &= T_{\text{HP},n_{\text{HP}}}^{\text{out}}; \\ T_{\text{MS}}^{S,\text{out}} &= T_{\text{MS}}^{S,\text{in}}, \end{aligned} \tag{21}$$

$$T_{\text{MS}}^{W,\text{out}} = T_{\text{MS}}^{W,\text{in}}, \tag{22}$$

where x^{in} is inlet vapor fraction of the moisture separator, x^{out} is outlet vapor fraction of the moisture separator, P_{T1}, P_{T2}, P_{T3}, P_{T4} are coefficients obtained from the producer.

3.1.5. Reheater

The quality of the steam at the outlet of the HP part is much lower than at the inlet. In order to obtain as much power as possible in the next stages it is not enough to dry the wet steam. In this case the steam should also be heated up in the reheater, e.g. by using the live steam from the turbine inlet or one of the vents. The reheater outlet mass flow rate M_R^{out} and the outlet pressure P_R^{out} are in linear relationship with its inlet values and coefficients of the proportionality are equal to the ratio of the nominal mass flow rate (23) and pressures (24) values respectively (see also Section 3.1.2). The outlet temperature T_R^{out} is approximated using Eq. (25) based on the construction data. Hence the reheater can be described in Eqs. (23)-(25) given below:

$$\begin{aligned} M_R^{\text{in}} &= M_{\text{MS}}^{S,\text{out}}; \\ M_R^{\text{out}} &= \frac{M_R^{\text{in}}}{M_R^{\text{nom,in}}} M_R^{\text{nom,out}}, \end{aligned} \tag{23}$$

$$\begin{aligned} P_R^{\text{in}} &= P_{\text{MS}}^{S,\text{out}}; \\ P_R^{\text{out}} &= \frac{P_R^{\text{in}}}{P_R^{\text{nom,in}}} P_R^{\text{nom,out}}, \end{aligned} \tag{24}$$

$$T_R^{\text{out}} = \left(H_T + I_T \frac{P_R^{\text{in}}}{P_R^{\text{nom,in}}} \right) T_R^{\text{nom,out}}, \tag{25}$$

where $M_R^{\text{nom,in}}$ is nominal steam mass flow rate at reheater inlet, $M_R^{\text{nom,out}}$ is nominal steam mass flow rate at reheater output, $P_R^{\text{nom,in}}$ is nominal steam pressure at reheater inlet, $P_R^{\text{nom,out}}$ is nominal steam pressure at reheater output, $T_R^{\text{nom,out}}$ is nominal steam temperature at reheater output, H_T, I_T are temperature coefficients of the reheater obtained from the steam turbine producer—Elbląg–Zamech.

3.1.6. Power

The power $N_{s,i}$ of each stage and the total theoretical power N_C are calculated from Eqs. (26) and (27).

$$N_{s,i} = \frac{k_{s,i}^{\text{nom}}}{\eta_{s,i}^{\text{nom}}} \frac{M_{s,i}^{\text{out}}}{M_{s,i}^{\text{nom,out}}} \frac{\Delta h_{s,i}^{\text{out}}}{\Delta h_{s,i}^{\text{nom,out}}} N_{s,i}^{\text{nom}} \qquad \text{for } s \in \{\text{HP}, \text{LP}\}, i \in \{1, \ldots, n_s\}, \tag{26}$$

$$N_C = \sum_{\substack{s \in \{\text{HP}, \text{LP}\} \\ i \in \{1, \ldots, n_s\}}}^{n_{\text{HP}}+n_{\text{LP}}} N_{s,i}, \tag{27}$$

where $\eta_{s,i}^{\text{nom}}$ is efficiency of the ith stage, $k_{s,i}^{\text{nom}}$ is power coefficient of the ith stage, $M_{s,i}^{\text{nom,out}}$ is nominal mass flow rate of the ith stage, $\Delta h_{s,i}^{\text{nom,out}}$ is theoretical enthalpy drop of the ith stage.

To obtain the effective power of the entire modeled steam turbine N_{Te} (Eq. (28)) the total theoretical power N_c is multiplied by the turbine efficiency η_e approximated with the function given in Eq. (29).

$$N_{\text{Te}} = N_C \frac{\eta_e}{\eta_e^{\text{nom}}}, \tag{28}$$

$$\eta_e = \eta_e^{\text{nom}} \left(\frac{N_C}{N_C^{\text{nom}}} \right)^{A_\eta \left(\frac{N_C^{\text{nom}}}{N_C} \right)^2}, \tag{29}$$

where η_e^{nom} is nominal turbine efficiency, N_C^{nom} is nominal total power, A_η is efficiency coefficient.

3.2. Dynamic model

The static model can be successfully used to analyze the static states. However, there is a need to study the behavior of the steam turbine also in transient states, e.g. for control and diagnostic purposes, and in this case only the dynamic model can be used. To meet this, the dynamic model of the turbine is proposed.

Similar to the static model the inputs to the model are: steam mass flow rate M, pressure P, and temperature T, and the reference valve opening degree α_{CV}^i. The outputs from the model are: output mass flow rates of the stages, output pressures of the stages, output temperatures of steam in most of sub models, enthalpy drops along stages, power of each stage and total power of steam turbine.

3.2.1. Control valve

The input to the control valve element is the reference valve opening degree α_{CV}^i. Taking into account common construction of the valve actuator, the control valve with current opening degree α_{CV}^0 as output is modeled as inertial element with the gain coefficient k_{CV} and the time constant τ_{CV} (30). The mass flow rate $M_{\text{CV}}^{\text{out}}$ at the outlet of the valve is proportional to the product of their inlet pressure P and current valve opening degree α_{CV}^0 (see Eq. (1) in Section 3.1). The pressure at the outlet of the valve is modeled as proportional to the current valve opening degree α_{CV}^0 (see Eq. (2) in Section 3.1).

$$\tau_{\text{CV}} \frac{d\alpha_{\text{CV}}^0}{dt} + \alpha = k_{\text{CV}} \alpha_{\text{CV}}^i, \tag{30}$$

where k_{CV} is inertia gain, τ_{CV} is inertia time constant.

3.2.2. Dead space

In the dynamic model of this element relationship between the mass flows at the inlet and the outlet remains the same like in the static model (5). The behavior of the element on the path of pressure is modeled as an integral element with the time constant of integration $\tau_{DS,s}$. The input to the element is difference of the mass flow rates at the inlet and outlet of the element. The mass flow rate $M^{out}_{DS,s}$ at the dead space outlet is equal to the mass flow rate $M^{in}_{DS,s}$ at its inlet (5). The output pressure $P^{out}_{DS,s}$ is calculated based on the pressure drop in the dead space given in Eq. (31) with time constant $\tau_{DS,s}$ (32). The dead space outlet temperature $T^{out}_{DS,s}$ can be calculated using the approximated function having the structure shown in Eq. (7). The calculations make use of the steam tables and the data given by the steam turbine producer in [20] in order to approximate presented functions.

$$\tau_{DS,s}\frac{dP^{out}_{DS,s}}{dt} = k_{DS,s}(M^{out}_{DS,s} - M^{out}_{s,1}) \qquad \text{for } s \in \{HP, LP\}, \tag{31}$$

$$\tau_{DS,s} = \frac{V_{DS,s}}{H_{DS,s}M^{nom,in}_{DS,s}v^{avg}_{DS,s}}^{\frac{1-H_{DS,s}}{H_{DS,s}}} \qquad \text{for } s \in \{HP, LP\}, \tag{32}$$

where $V_{DS,s}$ is accumulation volume of the dead space, $H_{DS,s}$ is adiabatic exponent of the dead space, $v^{avg}_{DS,s}$ is specific average steam volume of the dead space, $M^{nom,in}_{DS,s}$ is nominal input mass flow of the dead space, $k_{DS,s}$ is integral gain constant of the dead space.

3.2.3. Stages

Like in the static model, two types of stages are used in the dynamic model of the steam turbine. In the first type, the same relation for the mass flow rate is used as in the static model (8). However, due to dynamic character of the pressure drop, the relation for the output pressure is different. The pressure drop in each stage $P^{out}_{s,i}$ is described in Eq. (33).

For the low pressure part the vapor fraction $x_{s,i}$ is assumed to be a constant parameter, different for each stage. This assumption is justified by the small changes of vapor fraction in one stage (proof can be found in [5]). The steam temperature at the outlet of each stage is calculated using the estimated function based on the stage output pressure $P^{out}_{s,i}$, the same as in the static model given in Eqs. (11)–(13). The estimation makes use of the factory data and the steam tables.

$$\tau_{s,i}\frac{dP^{out}_{s,i}}{dt} = k_{s,i}(M^{out}_{s,i} - M^{in}_{s,i}) \qquad \text{for } s \in \{HP, LP\}, \tag{33}$$

where

$$\tau_{s,i} = \frac{V_{s,i}}{M^{out}_{s,i}}\frac{1}{H_{s,i}v^{nom}_{s,i}} + \frac{P^{nom}_{s,i}(1-x_{s,i})}{v''_{s,i}r_{s,i}}D_{s,i} \qquad \text{for } s \in \{HP, LP\}, i \in \{1, \dots, n_s\}, \tag{34}$$

$$D_{s,i} = \frac{D_D}{E_D\left(\sqrt{F_D + G_D P^{in}_{s,i}} - H_D\right) + I_D P^{in}_{s,i}} \qquad \text{for } s \in \{HP, LP\}, i \in \{1, \dots, n_s\}, \tag{35}$$

$$r_{s,i} = J_r + \frac{K_r}{L_r + P_{s,i}} \qquad \text{for } s \in \{HP, LP\}, i \in \{1, \dots, n_s\}, \tag{36}$$

$$x_{s,i} = A_{x,s,i} - B_{x,s,i}\frac{P^{in}_{s,i}}{P^{nom,in}_{s,i}} \qquad \text{for } s \in \{HP, LP\}, i \in \{1, \dots, n_s\}, \tag{37}$$

where $P^{nom,in}_{s,i}$ is nominal inlet pressure of the ith stage, $V_{s,i}$ is accumulation volume of the ith stage, $H_{s,i}$ is adiabatic exponent of the ith stage, $v^{nom}_{s,i}$ is nominal specific volume of the ith stage, $v''_{s,i}$ is average specific volume of the ith stage for the degree of dryness equal to one, D_D, E_D, F_D, G_D, H_D, I_D, J_r, K_r, L_r are coefficients of function $D_{s,i}$ and $r_{s,i}$ (estimated with usage of the steam tables based on information from the producer), $A_{x,s,i}$, $B_{x,s,i}$ are temperature function coefficients of ith stage, $k_{s,i}$ is integral gain constant of ith stage of sth ST section.

In case of stages with the vents the steam mass flow rate $M^{out}_{Vent,s,i}$ at vent outlet is calculated as a proportion given in Eq. (9), based on the assumption of rough relation to the nominal value in even steam flow distribution between the next stage and the vent.

3.2.4. Moisture separator and reheater

The moisture separator and the reheater are treated in the presented model as one device, with no pressure drop in the pipelines in front of the separator and between the separator and the reheater. The mechanical separator itself does not generate any pressure nor temperature drop of the steam and the condensate. The relations remain the same as in the static model. Because of that, the output steam pressure $P^{S,out}_{MS}$ and the condensate pressure $P^{W,out}_{MS}$ are equal to the HP part output pressure $P_{n_{HP}}$, Eqs. (19) and (20). Similarly, the output steam temperature $T^{S,out}_{MS}$ and the condensate temperature $T^{W,out}_{MS}$ are equal to the HP part output temperature $T_{n_{HP}}$, Eqs. (21) and (22).

The steam mass flow rate $M_{MS}^{S,out}$ at moisture separator outlet is calculated using the degree of dryness x_n of the last stage of the HP part, and its mass flow rate $M_{MS}^{S,in}$, Eq. (15). The condensate mass flow rate $M_{MS}^{W,out}$ is calculated as a complement to the output steam mass flow rate $M_{MS}^{S,out}$ (16). These relations are supported by the experts knowledge.

The reheater situated behind the moisture separator is characterized by the pressure drop P_R, which can be described in Eq. (38) with time constant τ_R (39). The reheater output mass flow rate M_R^{out} is proportional to the separator output mass flow rate $M_{MS}^{S,out}$, Eq. (23). The reheater output temperature T_R^{out} is given in Eq. (25), based on the estimated function defined by the design and technology of the reheater, and supported by the factory data.

$$M_R^{in} = M_{MS}^{S,out}; \ \tau_R \frac{dP_R^{out}}{dt} = k_R (M_R^{in} - M_{LP,1}^{out}), \tag{38}$$

$$\tau_R = \frac{V_R}{H_R^{avg} M_R^{nom,\ out} \upsilon_R^{avg}} \left(\frac{P_R^{out}}{P_R^{nom,out}} \right)^{\frac{1-H_R}{H_R}}, \tag{39}$$

where $M_R^{nom,out}$ is nominal reheater output mass flow rate, $P_R^{nom,out}$ is nominal reheater output pressure, H_R^{avg} is average adiabatic exponent of the reheater, V_R is reheater accumulation volume, υ_R^{avg} is average specific volume of the reheater, k_R is integral gain constant.

3.2.5. Power

The power of the steam turbine in case of the dynamic model is calculated in the same way as in the static model. In order to calculate it in each stage, the enthalpy drop $\Delta h_{s,i}^{out}$ is calculated from Eq. (14) based on the stage input pressure $P_{s,i}^{in}$, the stage output pressure $P_{s,i}^{out}$ and the input temperature $T_{s,i}^{in}$, [5].

In each stage, the stage power $N_{s,i}$ is calculated in the same way as in the static model (Eq. (26)), as shown in [5,6] for instance. The total theoretical power of the steam turbine N_C is the sum of elements $N_{s,i}$ (Eq. (27)). Similarly, the effective power is once again calculated the same way as in the static model based on Eqs. (28) and (29).

3.3. Simplified model

It is important for the model for control purposes to be as simple as possible, as its simplicity will ensure small computational complexity [20]. However, these simplifications should not affect significantly the model accuracy. Because of the complexity and computing requirements of the dynamic model presented in Section 3.2, a number of simplifications are proposed. For control purposes, there is no need to know the process variables at each possible turbine point, besides the controlled ones. In order to calculate only the most needed and characteristic variables, all stages were merged into sections called groups of stages. This approach enables to decrease the computational complexity by omitting the calculations of steam properties in each individual stage. The parameters, which remain to be calculated refer to most characteristic points and parameters, including: steam properties in the vicinity of vents, outputs of the HP and LP parts, inputs and outputs of the moisture separator and the reheater. Also the number of calculated enthalpies and total power components decreases, what makes the model less computationally complex.

3.3.1. Control valve

Valve opening degree with inertia α_{CV}^0 can be obtained by solving Eq. (30). Also an input pressure P_{CV}^{in} is equal to pressure P as in (2). The mass flow rate M_{CV}^{out} behind the control valve was calculated using Eq. (4) based on the de Saint–Venant–Wantzel equation. The output pressure needed to calculate the mass flow is equal to the CV input pressure P_{CV}^{out} (see Eq. (2)).

3.3.2. Dead space

Due to the influence of the reheater, the processes taking place in the dead space between the reheater and the LP part might be neglected. Regarding the dead space of HP part, the integral constant $\tau_{DS,s}$ in the dead space, was simplified to Eq. (40) instead of Eq. (32).

$$\tau_{DS,HP} = \frac{V_{DS,HP}}{H_{DS,HP} M_{HP,i}^{nom,in} \upsilon_{DS,HP}}, \tag{40}$$

where $M_{s,i}^{nom,in}$ is nominal inlet mass flow, $H_{DS,s}$ is adiabatic exponent, $V_{DS,s}$ is accumulation volume of the dead space, $\upsilon_{DS,s}$ is specific steam volume.

3.3.3. Stages

During the simplification process, the model parameters determined for each stage were averaged over the group of stages. The group of stages is understood as a number of stages situated between two adjacent vents, which are merged into the one stage. As a result, the mass flow rates of high pressure stages were calculated using the simplified form of the Stodola–Flügel cone law given in Eq. (41). In the presented case study, the error of the simplified Stodola–Flügel cone law is not greater than 0.3%, compared to the full cone law [4], which is sufficient for the purposes analyzed in the paper. Compared to the dynamic effects exerted by the reheater, additional dynamics introduced by the group of stages only contributes to the increase of the computational complexity. Because of that, the mass flow rate in the low pressure part was calculated based on the proportion expressed in Eq. (42) instead of Eq. (8), and the pressure in this part was calculated using Eq. (43) instead of Eqs. (33)-(37). In case of the temperature function, the averaging process changes its structure. The presented relation and structure result from calculations given in [4], supported by the interrelation between temperature and pressure characterizing the wet steam expansion process in the turbine. As a result the relations (11)-(13) are replaced by Eq. (44) and Eq. (45) for the HP and LP part, respectively.

$$M_{\mathrm{HP},j}^{\mathrm{out}} = M_{\mathrm{HP},j}^{\mathrm{nom,out}} \left(\frac{P_{\mathrm{HP},j}^{\mathrm{out}}}{P_{\mathrm{HP},j}^{\mathrm{nom,out}}} \sqrt{\frac{T_{\mathrm{HP},j}^{\mathrm{nom,out}}}{T_{\mathrm{HP},j}^{\mathrm{out}}}} \right), \quad j \in \{1, \ldots, m_s\}, \tag{41}$$

$$M_{\mathrm{LP},j}^{\mathrm{out}} = M_{\mathrm{LP},j}^{\mathrm{nom,out}} \frac{M_R^{\mathrm{out}}}{M_R^{\mathrm{nom,out}}}, \quad j \in \{1, \ldots, m_s\}, \tag{42}$$

$$P_{\mathrm{LP},j}^{\mathrm{out}} = P_{\mathrm{LP},j}^{\mathrm{nom,out}} \frac{P_R^{\mathrm{out}}}{P_R^{\mathrm{nom,out}}}, \quad j \in \{1, \ldots, m_s\}, \tag{43}$$

$$T_{\mathrm{HP},j}^{\mathrm{out}} = T_{\mathrm{HP},j}^{\mathrm{nom,out}} \left(T_{j,a1} + T_{j,b1} \sqrt{T_{j,c1} \frac{P_{\mathrm{HP},n_{\mathrm{LP}}}^{\mathrm{out}}}{P_{\mathrm{HP},n_{\mathrm{LP}}}^{\mathrm{nom,out}}} - 1} \right), \quad j \in \{1, \ldots, m_s\}, \tag{44}$$

$$T_{\mathrm{LP},j}^{\mathrm{out}} = T_{\mathrm{LP},j}^{\mathrm{nom,out}} \left(T_{j,a2} + T_{j,b2} \sqrt{\frac{P_{\mathrm{LP},j}^{\mathrm{out}}}{P_{\mathrm{LP},j}^{\mathrm{nom,out}}}} \right), \quad j \in \{1, \ldots, m_s\}, \tag{45}$$

where $M_{\mathrm{HP},j}^{\mathrm{nom,out}}$ is nominal mass flow rate of the jth group of stages in HP part, $P_{\mathrm{HP},j}^{\mathrm{nom,out}}$ is nominal pressure of the jth group of stages in HP part, $T_{\mathrm{HP},j}^{\mathrm{nom,out}}$ is nominal temperature of the jth group of stages in HP part, $M_{\mathrm{LP},i}^{\mathrm{nom}}$ is nominal mass flow rate of the jth group of stages in LP part, $M_R^{\mathrm{nom,out}}$ is nominal reheater mass flow rate, $P_R^{\mathrm{nom,out}}$ is nominal average reheater pressure, $T_{j,a1}$, $T_{j,b1}$, $T_{j,c1}$, $T_{j,a2}$, $T_{j,b2}$ are temperature coefficients, $P_{\mathrm{LP},j}^{\mathrm{nom,out}}$ is nominal pressure of the jth group of stages in LP part, $P_{\mathrm{HP},n_{\mathrm{LP}}}^{\mathrm{nom,out}}$ is nominal pressure of the jth group of stages in HP part and the first and the last LP stage, $T_{\mathrm{LP},j}^{\mathrm{nom,out}}$ is nominal temperature of the jth group of stages in LP part.

3.4.3. Moisture separator and reheater

The relations for the extracted water in the moisture separator (Eqs. (17) and (18)) differ from Eqs. (16) and (22) due to utilizing of the approximation functions. The mass flow rate of the extracted water $M_{\mathrm{MS}}^{W,\mathrm{out}}$ was calculated using Eq. (17), assuming flow continuity in the moisture separator and taking into account the factory data given in [4]. The temperature of extracted water $T_{\mathrm{MS}}^{W,\mathrm{out}}$ was calculated using the relation (18), along with the factory data and the steam tables. Also τ_R in the reheater was defined in Eq. (46) instead of Eq. (39).

$$\tau_R = \frac{V_R}{H_R^{\mathrm{avg}} M_R^{\mathrm{nom,out}} v_R^{\mathrm{avg}}}, \tag{46}$$

where V_R is reheater accumulation volume, v_p^{avg} is average specific steam volume in the reheater, H_R^{avg} is average adiabatic exponent of the reheater, $M_R^{\mathrm{nom,out}}$ is nominal reheater mass flow rate.

3.4.4. Power

In case of the dynamic simplified model power is calculated like in the dynamic model. The only difference is that the calculations are performed using groups of stages instead of stages because of the simplification based on grouping the stages. The same relations dependent on the stages with their parameters include averaged parameters gained in the process of grouping.

4. Case study

The NPP steam turbine 4 CK 465 designed for the WWER-440/213 nuclear reactor serves as the reference plant for models examination. The total turbine power is 471.329 MW. The turbine consists of: HP part with ten stages and LP part with six stages, moisture separator and reheater (treated as one device) between HP and LP parts, and one control valve at the HP part inlet. Some stages were designed with extractions, which gives five vents in total, two in the HP part: stages 3 and 6, and three in the LP part: stages 2, 4, and 5. The steam properties (steam pressure, mass flow rate, temperature) are the model inputs and they are controlled by throttling by the control valve. The model enables to calculate steam pressure, mass flow rate, temperature, vapor fraction, theoretical power and enthalpy drop for each stage. Moreover, the temperature,

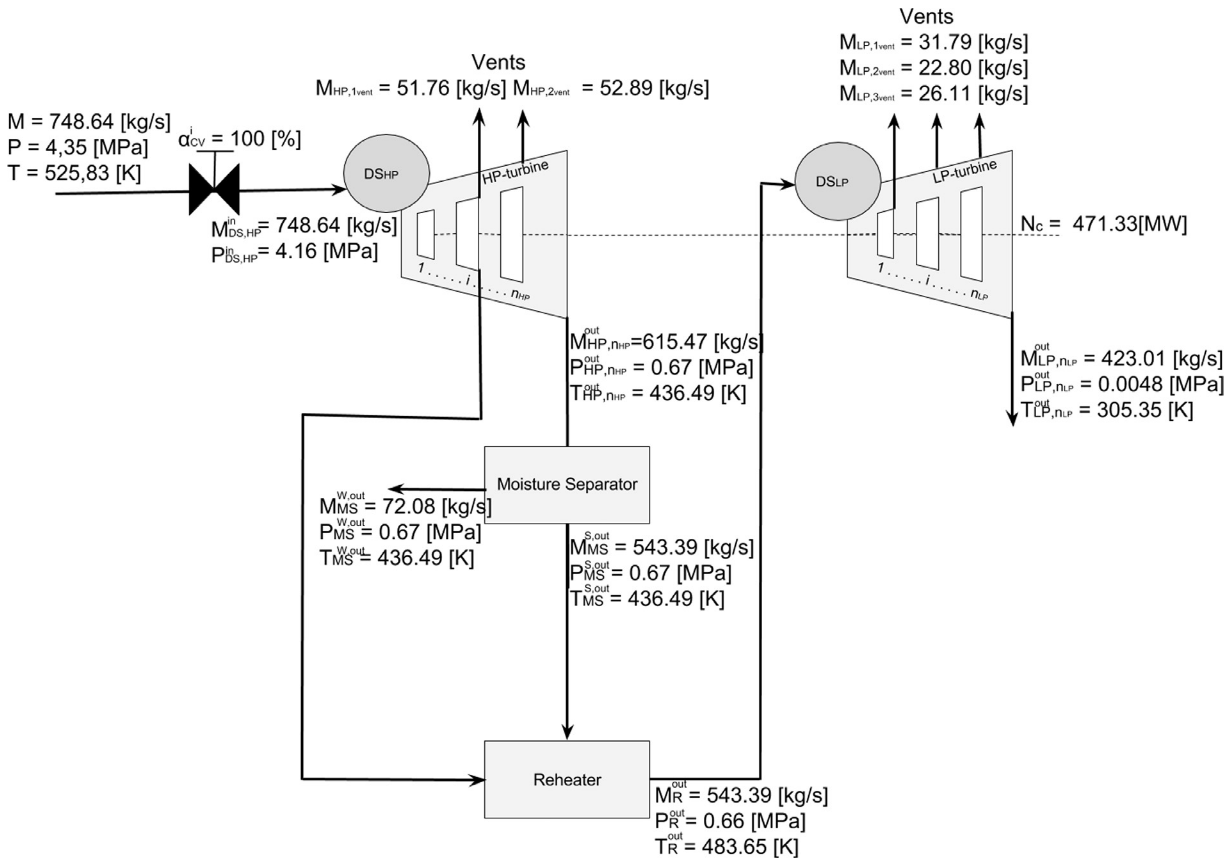

Fig. 2. Heat balance map for nominal operating point.

mass flow rate, and pressure are calculated for the moisture separator and the reheater. The powers, calculated for each stage, are used for calculating the overall turbine power. The heat balance map for the nominal operating point (valve opening degree equal to 100%) is presented in Fig. 2.

4.1. Simulation conditions

The models presented in the paper were implemented in Matlab®/Simulink®. The simulations were conducted on a personal class computer with Intel Core i5-3330 CPU 3.00 GHz, 3.20 GHz processor, 16 GB of RAM and Windows® 7 Professional operation system, with usage of 'ode3' solver based on Bogacki–Shampine formula, operating with fixed-step. The kind of solver as well as the step size used during the models simulation was carefully selected during the number of experiments carried out taking into account the models accuracy and computational load.

In Section 4.2 the simulation time steps of each model are compared and the resultant accuracies are analyzed. The analysis aimed at evaluating the influence of simulation time steps and the time of simulations.

The testing trajectory of the input signal that covers a wide range of operating conditions is presented in Fig. 3.

The models were assumed to start from the nominal value, therefore the initial conditions for each model were calculated for this operating point. The input signal (opening degree of the control valve) was expressed in percent, so the maximal opening of the control valve corresponds to the maximal power of the steam turbine at the nominal operation point, as defined by its construction in the designing process for the throttling control. The inlet pressure of the steam turbine for the maximal opening degree is equal to the nominal inlet pressure of 4.161 MPa.

4.2. Comparison of the models

The operations of the static, dynamic, and simplified dynamic models were simulated for the conditions described in Section 4.1. Because of the stage grouping in the simplified model, only the variables at the corresponding points in all models were the objects of comparison. A number of the common model points were chosen in order to present the most characteristic variables, such as pressure, mass flow rate, and temperature, complemented by the effective steam turbine power. These variables are compared in Figs. 4-16. The output pressure of the HP turbine part stage 3 is shown in

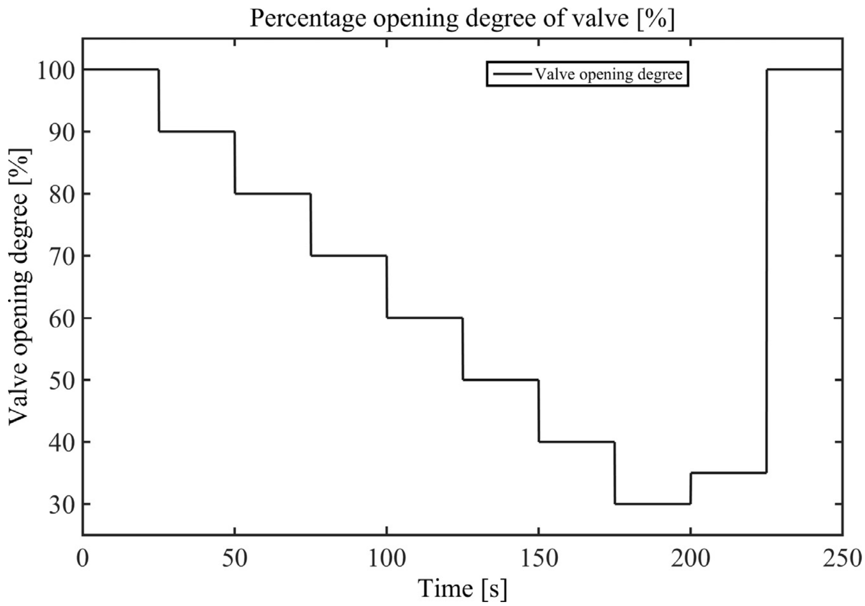

Fig. 3. Trajectory of steam turbine input signal.

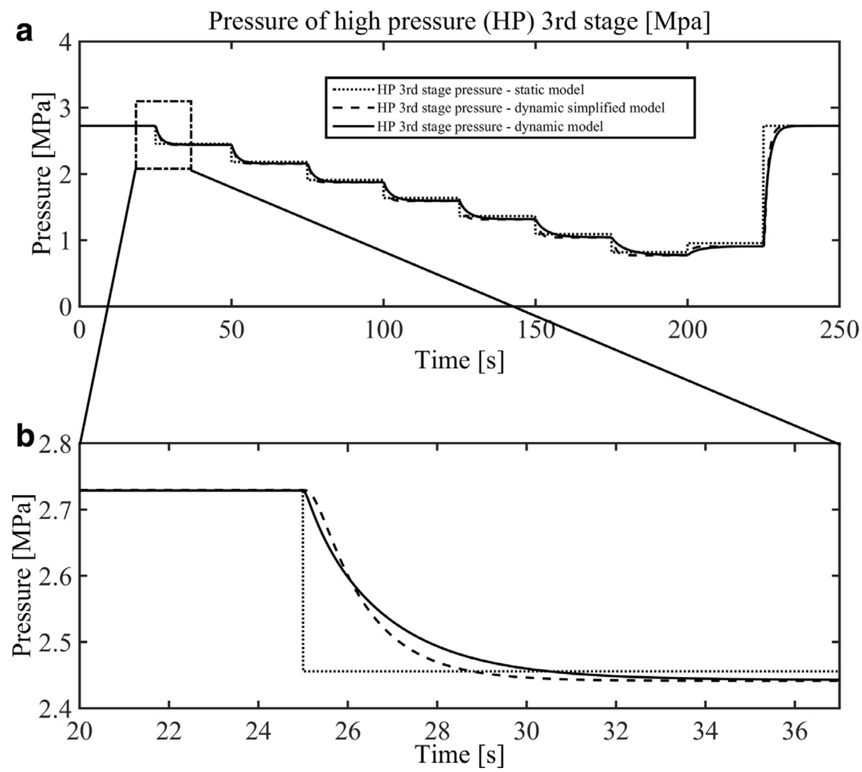

Fig. 4. Output steam pressure of the HP stage 3.

Fig. 4. Differences between the presented output pressure trajectories as generated by different models are mainly caused by different parameters used in the models.

For all three models, time step and its influence on the simulation results such as: calculation time of one iteration and therefore simulation time, was studied. The total time of conducting the simulation, for the run-time of 250 s and the selected simulation time step was measured with the real time system clock.

Table 1
Calculations time—models comparison.

Model type	Time step (s)	Calculation time (s)	Average time of one iteration (s)
Static	0.1	~7.95	0.0035
	0.0001	~7200	0.0029
Dynamic	0.0001	~13,620	0.0055
Simplified dynamic	0.1	~0.6832	0.0003
	0.0001	~7560	0.0030

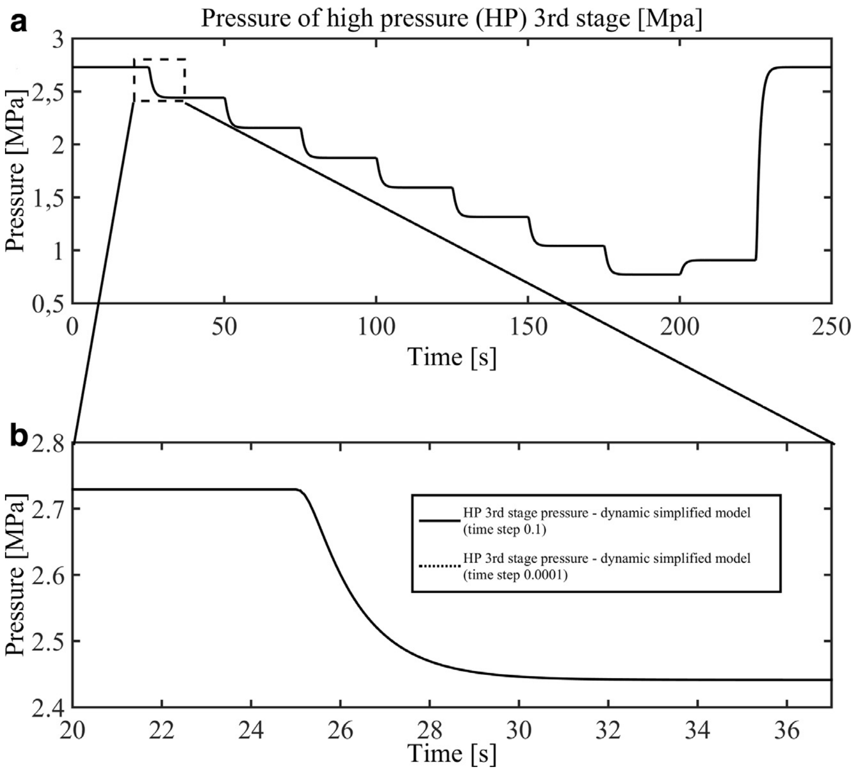

Fig. 5. Simplified dynamic model responses for different time steps (0.1 and 0.0001).

Due to the time scale of the dynamics of internal processes taking place in the turbine, the maximal time step for the dynamic model of steam turbine was assumed equal to $\Delta T_{s,\max}{}^{(d)} = 0.0001$ and for the same reason, the maximal time step for the simplified model was assumed equal to $\Delta T_{s,\max}{}^{(sd)} = 0.1$. The results of this study are shown in Table 1. Exceeding these values led to the solver instability during the simulation. From the other hand, utilization of the smaller time step by the solver does not improve the model accuracy, but leads to significant extending of the simulation time. For instance, Figs. 5-6 show the results of the simulations of the simplified dynamic model conducted for time steps equal 0.1 and 0.0001.

The comparison of all presented models calculated with the time step of 0.0001 is shown in Figs. 7-8, while the comparison of the simplified dynamic model calculated with the time step of 0.1 and the dynamic model calculated with the time step of 0.0001 is presented in Figs. 9-10. Each percentage residue was referenced to the value of the given model as the minuend in the difference.

Simulations carried out have showed that the static model and the simplified dynamic model can be used to calculate variables in the real time regime. The dynamic model without simplifications needs much more time to conduct the calculations, but it enables obtaining more detailed data across the steam turbine sections. The obtained results are collected in Table 1. Both dynamic models allow to observe transient states during turbine operation.

The constrains $\Delta T_{s,\max}{}^{(d)}$ and $\Delta T_{s,\max}{}^{(sd)}$ for the simulation time steps of the dynamic models appeared as a result of turbine dependencies and the accuracy of the solver used. When the time step limits were exceeded, the model became unstable. It is noteworthy that in the steady states the HP stage 3 output pressure converges to the same value.

The LP stage 2 output pressure is presented in Fig. 11. The parameters in the simplified model were averaged so the proportion based on these new parameters generated differences in the whole trajectory of the presented results.

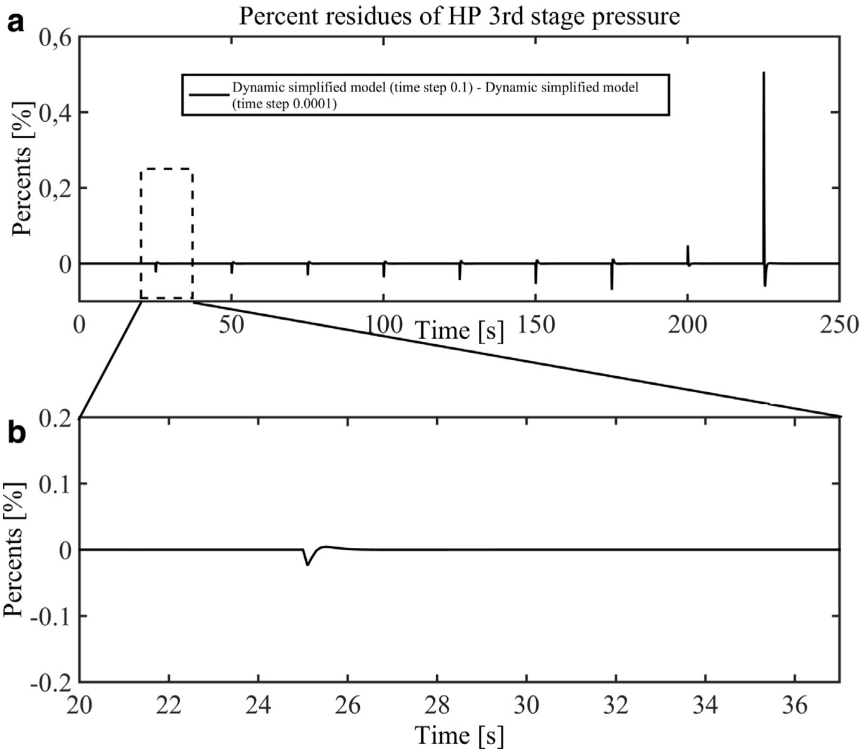

Fig. 6. Simplified dynamic model responses for different time steps (0.1 and 0.0001)—percentage residues.

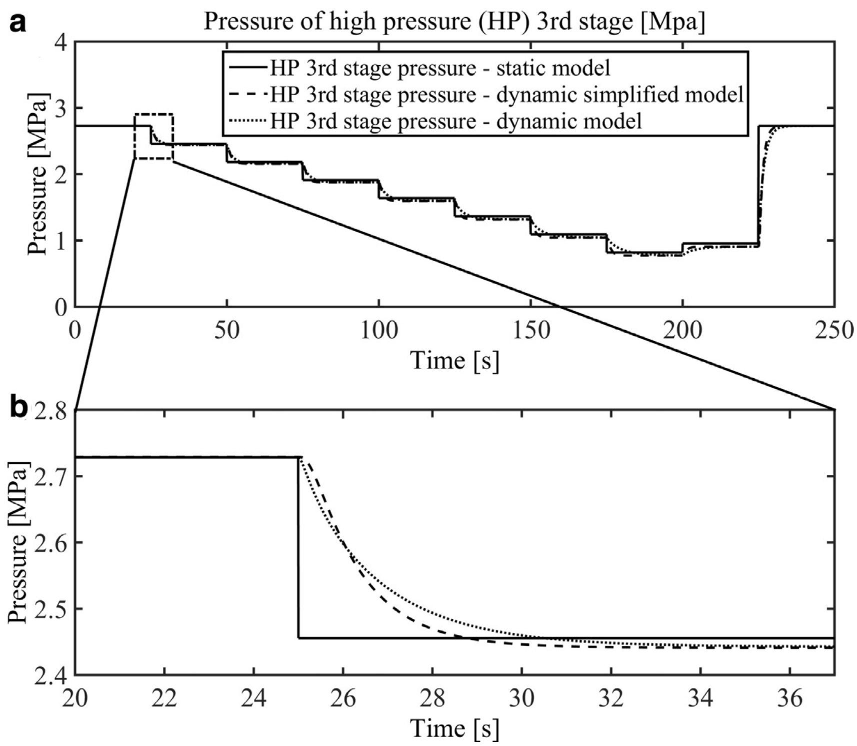

Fig. 7. Comparison of all presented models calculated with time step 0.0001.

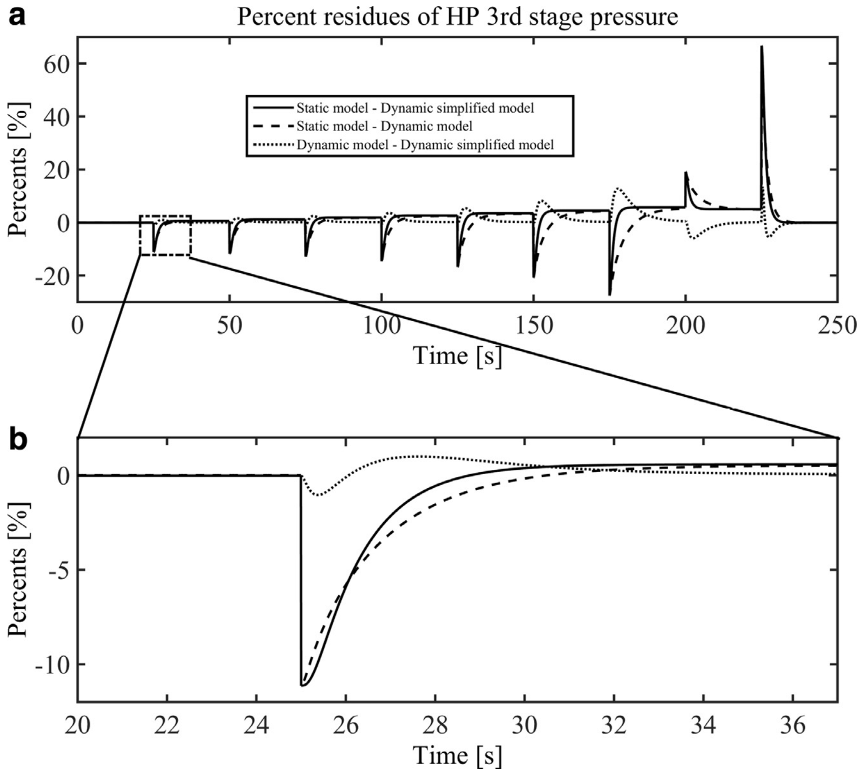

Fig. 8. Comparison of all presented models calculated with time step 0.0001—percentage residues.

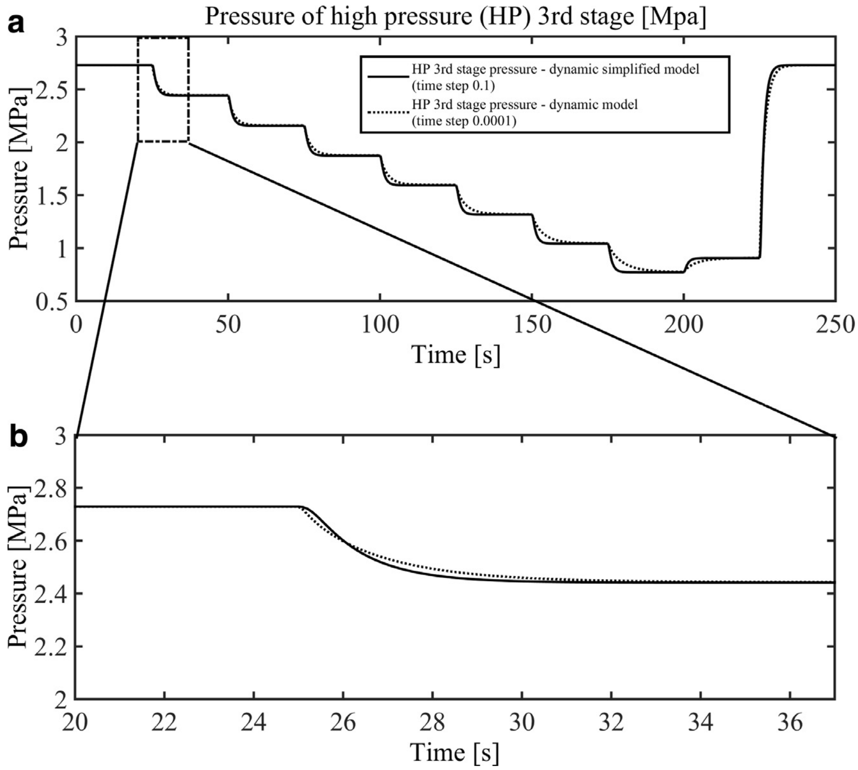

Fig. 9. Comparison of the simplified dynamic model calculated with time step 0.1 and the dynamic model calculated with time step 0.0001.

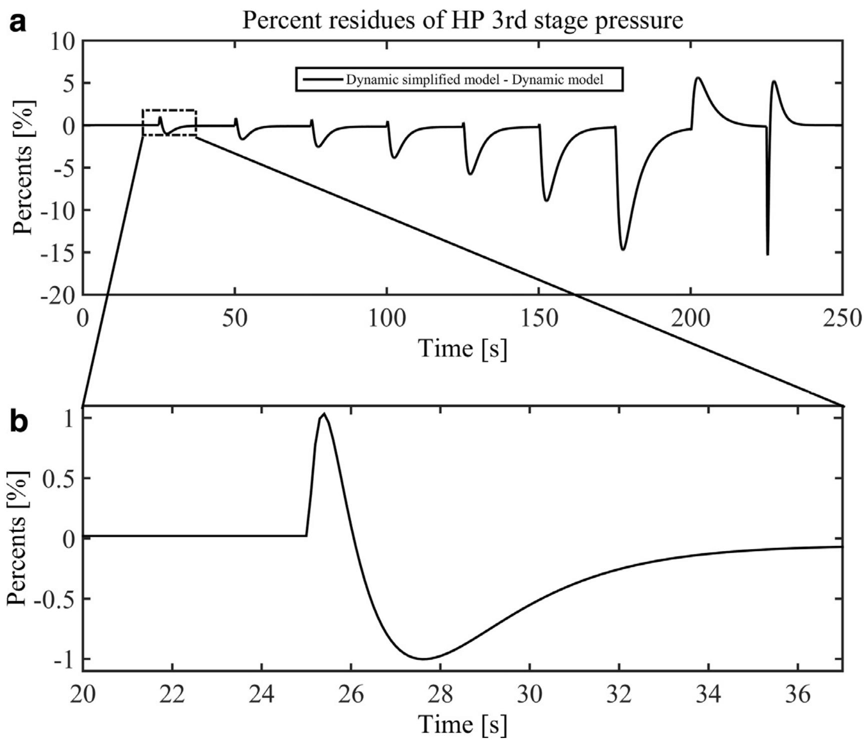

Fig. 10. Comparison of the simplified dynamic model calculated with time step 0.1 and the dynamic model calculated with time step 0.0001—percentage residues.

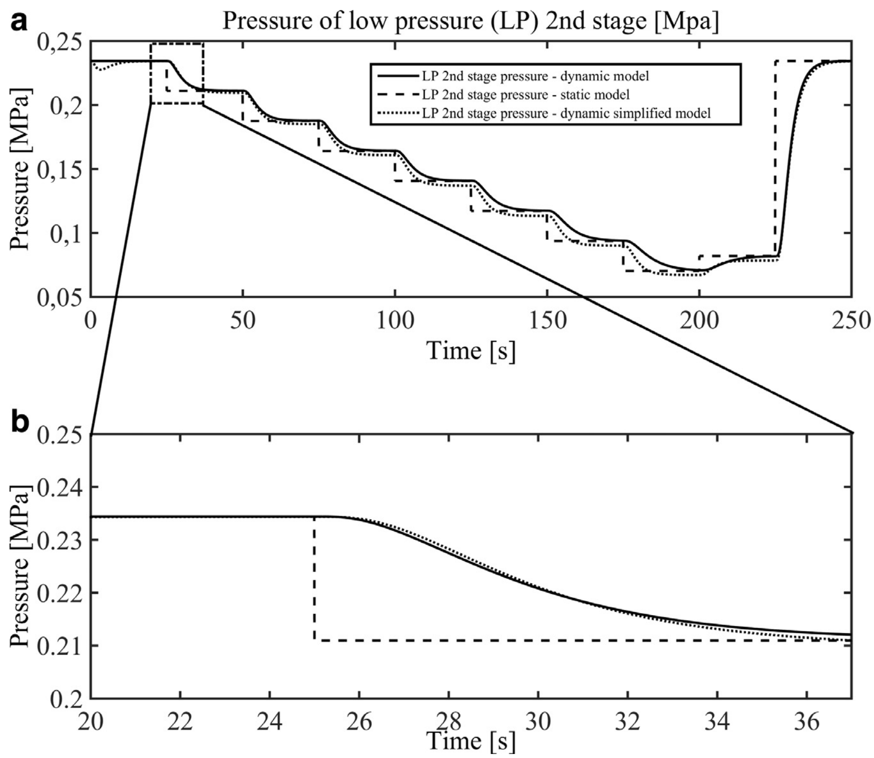

Fig. 11. Steam pressure at LP stage 2 outlet.

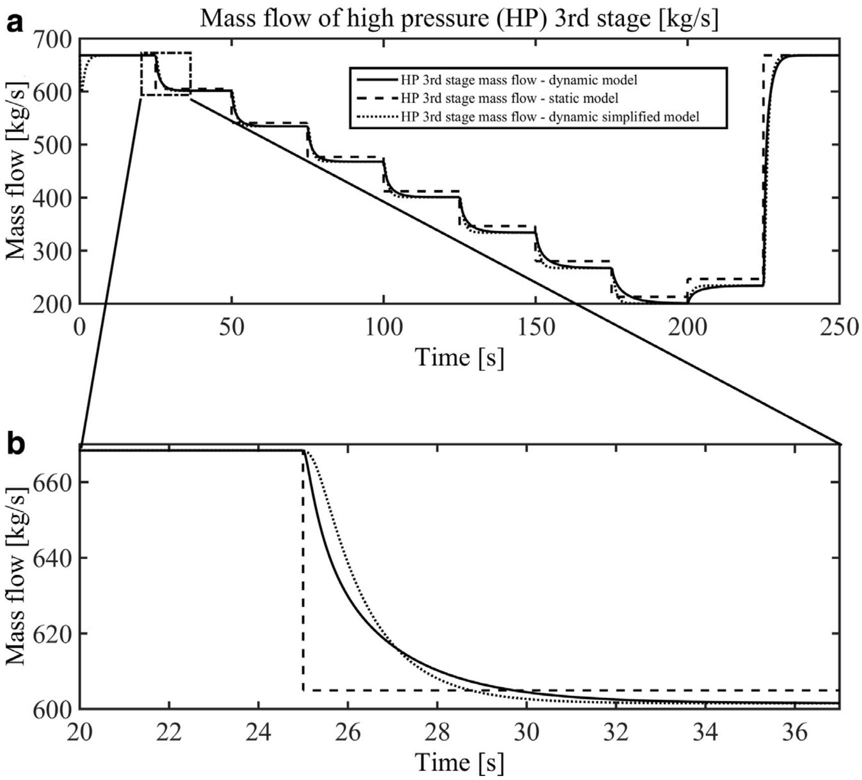

Fig. 12. Steam mass flow rate at HP stage 3 outlet.

As for the output, the HP stage 3 mass flow rate presented in Fig. 12 depends directly on the pressure (the Stodola–Flügel cone law) so the dynamic character of the pressure can be also seen in the trajectory of the mass flow rate in transient states.

In the LP part of the steam turbine, the stage 2 output mass flow rate reveals similar dynamic behavior as the pressure in this part. For simplified model the mass flow rate in this part was calculated as the proportion given in Eq. (42) based on the reheater mass flow rate. The trajectory of the steam mass flow rate at the LP stage 2 output is presented in Fig. 13.

The steam temperature at the HP stage 3 output is shown in Fig. 14. Differences between the presented models are caused by averaging parameters in the simplified model.

It results in slight differences even at the nominal point of the steam turbine operation. Also the steam temperature at the LP stage 2 output, presented in Fig. 15, reveals similar differences as the temperature in the HP part (see Eq. (45)).

The total effective power of the steam turbine is shown in Fig. 16. Its changes are generated by changing the input valve opening from 30 to 100% (Fig. 3). Despite the wide range of the changes, only slight differences between particular models can be observed.

Differences in the steam mass flow rates calculated by the particular models have significant impact on the effective power. Moreover, the factory parameters were averaged in the simplified model, thus contributing to additional effective power differences. The enthalpy drop in the dynamic model is calculated using Eq. (14) for the HP part, but in the LP part the pressure value used in Eq. (14) is given in Eq. (33). In the simplified model, the pressure in the LP part was calculated based on proportional relations (43). Moreover, the enthalpy drop was calculated using Eq. (14).

Regarding the static model, its results strongly depend on the given nominal values of the steam turbine. A characteristic property of the model can be observed for almost each variable, namely according to experimental data [15] the farther from the nominal point is the operational point, the less accurate is the model when calculating the static states.

As it can be seen in Table 2, the dynamic model results are closer to the reference data [19]. Unfortunately only selected operating points of reference data were available so comparison of other variables trajectories with the reference data was impossible in this case. The static model presents a good convergence of the process in the steady states, but the missing dynamic relations make it slightly less accurate, compared to the dynamic models. As could be expected, the simplified dynamic model is slightly less accurate than the full dynamic model. Along with the simplifications of power coefficient calculations for group of stages, the sources of the observed differences could be the rounding errors and the computational accuracy of the software. Nonetheless the simplified dynamic model enables to receive results with high accuracy at much lower computational cost, compared to the full dynamic model.

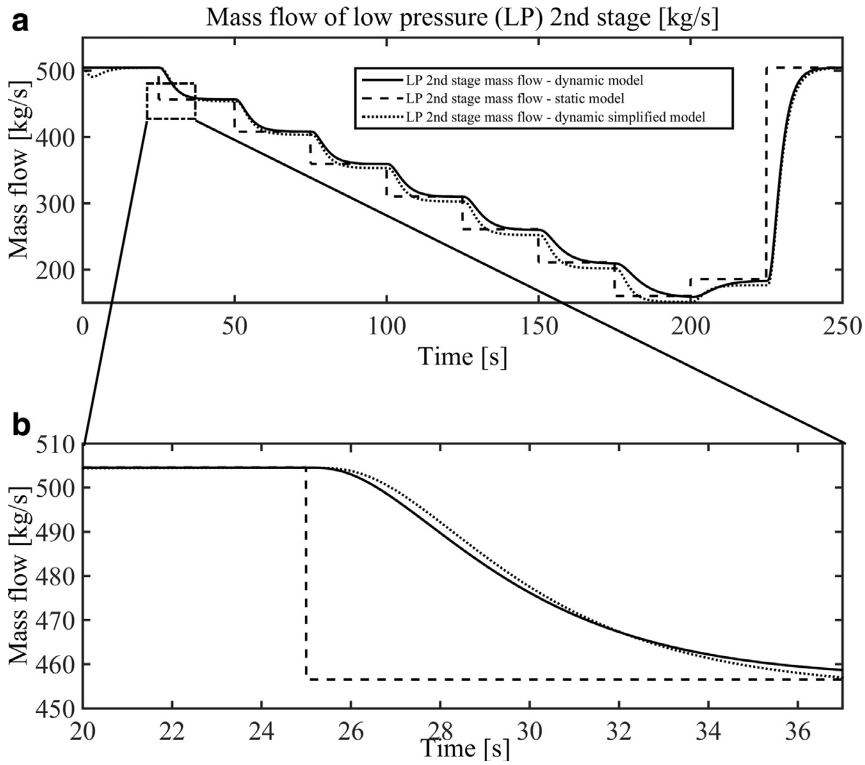

Fig. 13. Steam mass flow rate at LP stage 2 outlet.

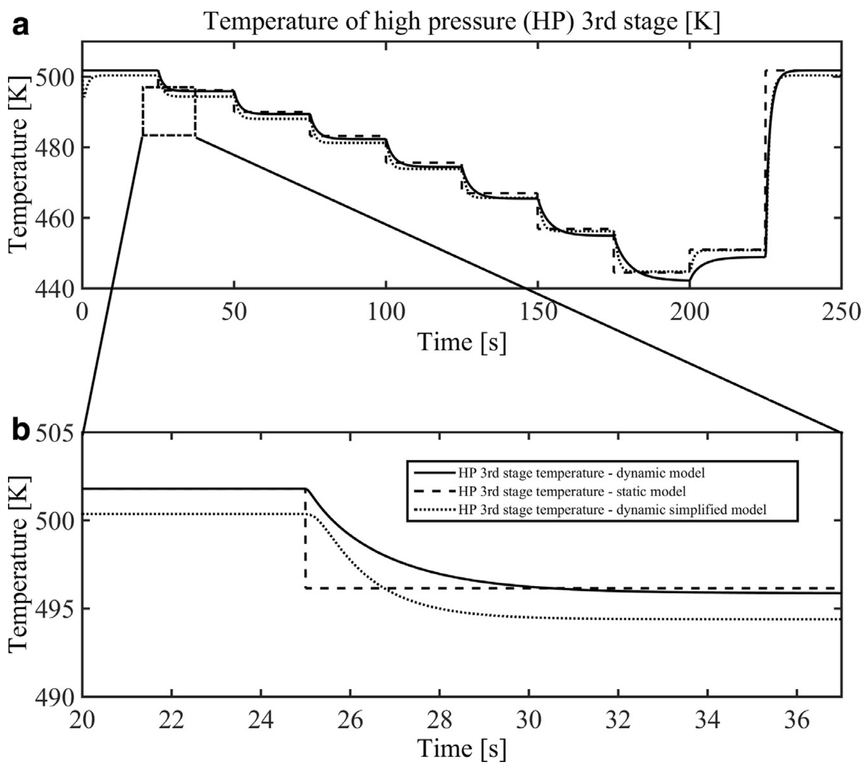

Fig. 14. Steam temperature at HP stage 3 outlet.

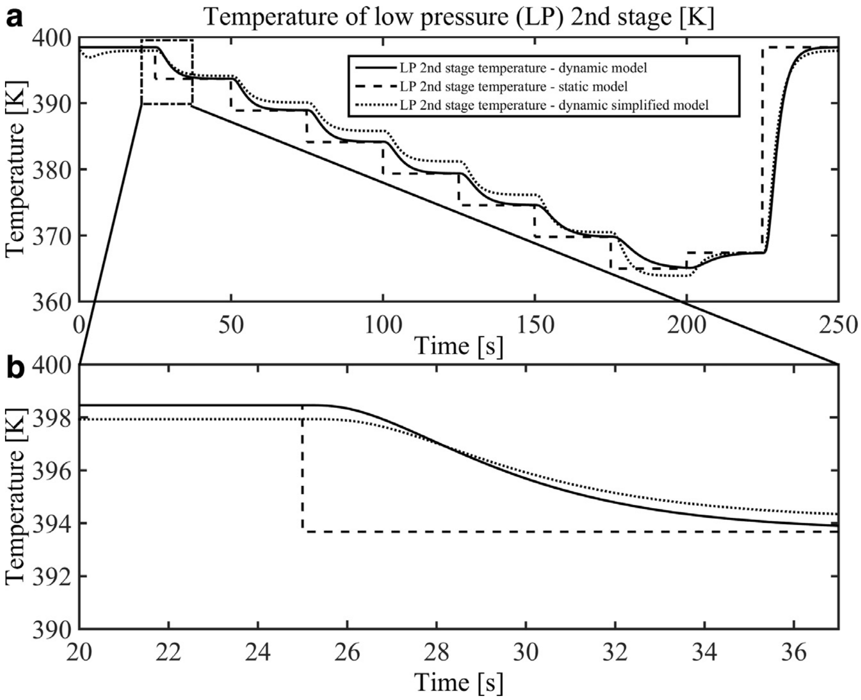

Fig. 15. Steam temperature at LP stage 2 outlet.

Table 2
Power percentage: experimental data and model calculations (steady states).

Input power (%)	Reference data Power (%)	Static model Power (%)	Squared error Power (%)	Dynamic model Power (%)	Squared error Power (%)	Simplified dynamic model Power percentage (%)	Squared error Power (%)
100	100.00	100.00	0	100.00	0	100.00	0
90	89.23	87.87	1.84	89.34	0.01	88.85	0.15
75	73.25	70.66	6.71	73.50	0.06	72.58	0.45
50[a]	46.88	48.48	2.57	49.77	8.35	47.69	0.65
30[a]	23.79	28.56	22.79	31.76	63.50	29.24	29.67

[a] Reference data in these points were obtained in different control conditions.

5. Conclusions

The paper analyzes three multivariable, nonlinear models of the nuclear power plant steam turbine. One of them is static, while two others are dynamic.

Regarding the dynamic models, both of them enable to calculate transient states at the output of the steam turbine and its internal variables.

The dynamic model is characterized by high computational complexity caused by its detailed structure, in which each single stage is modeled. This computational complexity, in combination with the small time step used by the solver during the simulations, ensures very good accuracy, therefore this model can be considered as the reference model. It also provides opportunities to study the variables inside the steam turbine and their dynamics, fully modeled using 111 process variables. However, due to a relatively long time required for calculations, this model cannot be used for on-line control purposes.

Unlike the dynamic model with stage-by-stage turbine modeling, the simplified dynamic model can be utilized for on-line control purposes, e.g. for model predictive control. This advantage is a result of introduced simplifications, which remarkably decreased the computational complexity, while only slightly decreased the accuracy. This model also provides access to the most characteristic internal variables (52 process variables).

The static model also enables to calculate output and internal variables (108 process variables), but only in the steady states.

The models were verified on the case study, in which the modeled turbine was the steam turbine 4CK465 designed for the WWER-440/213 reactor. The general behavior and certain differences between these models are shown in the figures and collected in the tables. As expected, in the steady states the output variables of the examined models have similar values, but significantly differ in the transient conditions.

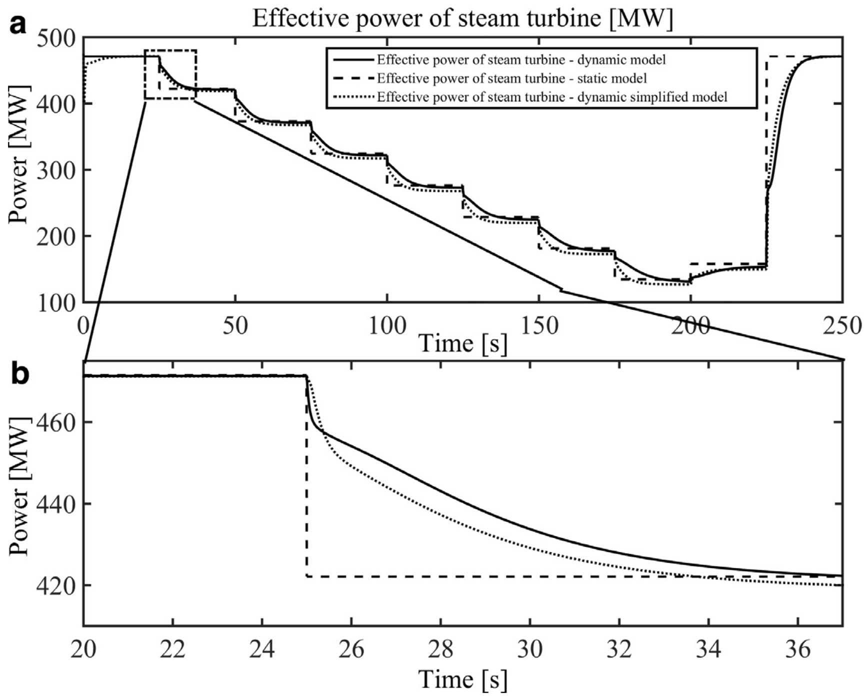

Fig. 16. Total effective power of steam turbine.

Current authors research activities focus on developing the steam turbine model that will reflect, with a satisfying accuracy, all collected and internal variables, which are necessary for control purposes, at minimal computational burden, enabling on-line calculation. Such a model can be used for on-line model based control, e.g. model predictive control. Preliminary analyses have led the authors to focus on the gray-box modeling approach with utilization of data driven techniques, such as neural networks and fuzzy logic. Another promising research topic is fractional order steam turbine modeling, that has been successfully applied to modeling neutron point kinetics and heat exchange in nuclear reactor [21,22]. More detailed model can be also used for the purposes of diagnostic and monitoring. Authors are looking forward to develop diagnostic system which would be useful for the purposes of fault tolerant control [23].

Acknowledgments

This work was supported by the National Centre for Research and Development under Strategic Research Project: "Technologies for the development of safe nuclear energy" – Research Task No. 10 entitled: 'Development and implementation of an exemplary method of system analysis of the nuclear power plant with light water reactor in partial cogeneration work. The National Center for Research and Development research project for years 2012–2014—in Polish No. SP/J/10/176450/12. The authors wish to express their thanks for the support.

It was also supported by the European Union project "INSPE—INNOVATIVE NUCLEAR AND SUSTAINABLE POWER ENGINEERING". The authors wish to express their thanks for the support.

Appendix

Table A.1
Parameters in the developed models.

Parameter name			Symbol	Value	Units
Accumulation volume	High pressure section	Dead space	$V_{DS,s}$	4	m^3
		1st stage	$V_{s,i}$	0.03	m^3
		2nd stage		0.04	m^3
		3rd stage		65	m^3
		4th stage		0.045	m^3
		5th stage		0.052	m^3

(*continued on next page*)

Table A.1 (*continued*)

Parameter name			Symbol	Value	Units
		6th stage		65	m^3
		7th stage		0.066	m^3
		8th stage		0.068	m^3
		9th stage		0.078	m^3
		10th stage		0.084	m^3
	Reheater	V_R		470.000	m^3
	Low pressure section	Dead space	$V_{DS,s}$	10.000	m^3
		1st stage	$V_{s,i}$	0.192	m^3
		2nd stage		40	m^3
		3rd stage		0.360	m^3
		4th stage		50	m^3
		5th stage		60	m^3
		6th stage		15	m^3
Specific steam volume	High pressure section	Dead space	$\upsilon_{DS,s}^{avg}$	0.046	m^3/kg
		1st stage	$\upsilon_{s,i}^{nom}$	0.054	m^3/kg
		2nd stage		0.060	m^3/kg
		3rd stage		0.070	m^3/kg
		4th stage		0.082	m^3/kg
		5th stage		0.094	m^3/kg
		6th stage		0.110	m^3/kg
		7th stage		0.140	m^3/kg
		8th stage		0.170	m^3/kg
		9th stage		0.210	m^3/kg
		10th stage		0.250	m^3/kg
	Reheater		v_R	0.285	m^3/kg
	Low pressure section	Dead space	$\upsilon_{DS,s}^{avg}$	0.320	m^3/kg
		1st stage	$\upsilon_{s,i}^{nom}$	0.500	m^3/kg
		2nd stage		0.780	m^3/kg
		3rd stage		1.400	m^3/kg
		4th stage		2.500	m^3/kg
		5th stage		6.400	m^3/kg
		6th stage		26.000	m^3/kg
Adiabatic exponent	High low pressure section	Dead space	$H_{DS,s}$	1.164	–
		1st stage	$H_{s,i}$	1.133	–
		2nd stage		1.333	–
		3rd stage		1.132	–
		4th stage		1.131	–
		5th stage		1.131	–
		6th stage		1.130	–
		7th stage		1.129	–
		8th stage		1.128	–
		9th stage		1.127	–
		10th stage		1.126	–
	Reheater		H_R	1.200	–
	Low pressure section	Dead space	$H_{DS,s}$	1.300	–
		1st stage	$H_{s,i}$	1.300	–
		2nd stage		1.300	–
		3rd stage		1.134	–
		4th stage		1.131	–
		5th stage		1.129	–
		6th stage		1.125	–
Mass flow rate	High pressure section	Dead space	$M_{DS,s}^{nom,in}$	748.638	kg/s
		1st, 2nd, 3rd stage	$M_{s,i}^{nom,out}$	748.638	kg/s
		4th, 5th, 6th stage		668.365	kg/s
		7th, 8th, 9th, 10th stage		615.474	kg/s
	Reheater		M_R^{nom}	504.510	kg/s
	Low pressure section	Dead space 1st, 2nd stage	$M_{s,i}^{nom,out}$	504.510	kg/s
		3rd, 4th stage		472.726	kg/s
		5th stage		449.920	kg/s
		6th stage		423.006	kg/s
	Vents	1st extraction	$M_{s,i_{vent}}^{nom,out}$	51.758	kg/s
		2nd extraction		52.891	kg/s
		3rd extraction		31.788	kg/s
		4th extraction		22.802	kg/s
		5th extraction		26.110	kg/s
	Separator	Steam	$M_{MS}^{nom,S,in}$	543.392	kg/s
Pressure	High pressure section	Dead space	$P_{DS,s}^{nom,out}$	4.1610	MPa

(*continued on next page*)

Table A.1 (*continued*)

Parameter name			Symbol	Value	Units
		1st stage	$P_{s,i}^{\text{nom,out}}$	3.6433	MPa
		2nd stage		3.1687	MPa
		3rd stage		2.7285	MPa
		4th stage		2.3509	MPa
		5th stage		1.9999	MPa
		6th stage		1.6729	MPa
		7th stage		1.3723	MPa
		8th stage		1.1065	MPa
		9th stage		0.8741	MPa
		10th stage		0.6724	MPa
	Reheater		$P_{R}^{\text{nom,out}}$	0.6449	MPa
			$P_{R}^{\text{nom,in}}$	0.6724	MPa
	Low pressure section	Dead space	$P_{\text{DS},s}^{\text{nom,out}}$	0.6449	MPa
		1st stage	$P_{s,i}^{\text{nom,out}}$	0.3900	MPa
		2nd stage		0.2344	MPa
		3rd stage		0.1200	MPa
		4th stage		0.0762	MPa
		5th stage		0.0287	MPa
		6th stage		0.0048	MPa
	Separator		$P_{\text{MS}}^{S,\text{nom}}$	0.6586	MPa
Temperature	High pressure section	Dead space	$T_{\text{DS},s}^{\text{nom}}$	525.83	K
		1st stage	$T_{s,i}^{\text{nom,in}}$, $T_{s,i}^{\text{nom,out}}$	518.00	K
		2nd stage		510.04	K
		3rd stage		501.79	K
		4th stage		493.84	K
		5th stage		485.52	K
		6th stage		476.68	K
		7th stage		467.16	K
		8th stage		457.48	K
		9th stage		447.29	K
		10th stage		436.49	K
	Reheater		$T_{R}^{\text{nom,out}}$	483.65	K
	Low pressure section	Dead space	$T_{\text{DS},s}^{\text{nom}}$	483.65	K
		1st stage	$T_{s,i}^{\text{nom,in}}$, $T_{s,i}^{\text{nom,out}}$	438.15	K
		2nd stage		398.46	K
		3rd stage		383.57	K
		4th stage		365.45	K
		5th stage		341.25	K
		6th stage		305.35	K
Temperature function coefficients, dryness coefficients	Dead space, high pressure section, low pressure section		A_{DS}, A_T	453.03	=
			$\text{B}_{\text{DS}}, B_T$	0.096	=
			C_{DS}, C_T	0.0596	=
	Reheater		H_T	0.88	=
			I_T	0.12	=
	High pressure section	1st stage	$A_{x,s,i}$	0.996	=
			$B_{x,s,i}$	0.0100	=
		2nd stage	$A_{x,s,i}$	0.990	=
			$B_{x,s,i}$	0.0190	=
		3rd stage	$A_{x,s,i}$	0.984	=
			$B_{x,s,i}$	0.0255	=
		4th stage	$A_{x,s,i}$	0.977	=
			$B_{x,s,i}$	0.0320	=
		5th stage	$A_{x,s,i}$	0.970	=
			$B_{x,s,i}$	0.0375	=
		6th stage	$A_{x,s,i}$	0.963	=
			$B_{x,s,i}$	0.0418	=
		7th stage	$A_{x,s,i}$	0.958	=
			$B_{x,s,i}$	0.0455	=
		8th stage	$A_{x,s,i}$	0.951	=
			$B_{x,s,i}$	0.0485	=
		9th stage	$A_{x,s,i}$	0.942	=
			$B_{x,s,i}$	0.0508	=
		10th stage	$A_{x,s,i}$	0.934	=
			$B_{x,s,i}$	0.0520	=
	Efficiency		A_{η}	0.003	=

(*continued on next page*)

Table A.1 (*continued*)

Parameter name			Symbol	Value	Units
Theoretical enthalpy drop	High pressure section	1st stage	$\Delta h_{s,i}^{nom,out}$	26.10	kJ/kg
		2nd stage		27.12	kJ/kg
		3rd stage		28.73	kJ/kg
		4th stage		28.25	kJ/kg
		5th stage		30.26	kJ/kg
		6th stage		32.90	kJ/kg
		7th stage		35.85	kJ/kg
		8th stage		38.23	kJ/kg
		9th stage		40.97	kJ/kg
		10th stage		44.49	kJ/kg
	Low pressure section	1st stage		94.43	kJ/kg
		2nd stage		98.26	kJ/kg
		3rd stage		89.20	kJ/kg
		4th stage		97.42	kJ/kg
		5th stage		145.27	kJ/kg
		6th stage		232.8	kJ/kg
Power coefficient	High pressure section	1st stage	$k_{s,i}^{nom}$	0.0370	–
		2nd stage		0.0384	–
		3rd stage		0.0408	–
		4th stage		0.0346	–
		5th stage		0.0370	–
		6th stage		0.0403	–
		7th stage		0.0387	–
		8th stage		0.0412	–
		9th stage		0.0442	–
		10th stage		0.0480	–
	Low pressure section	1st stage		0.0862	–
		2nd stage		0.0927	–
		3rd stage		0.0811	–
		4th stage		0.0887	–
		5th stage		0.1154	–
		6th stage		0.01357	–
Nominal total power			N_C^{nom}	471.329	MW
Nominal turbine efficiency			η_e^{nom}	0.863	–
Efficiency	High pressure section	1st, 2nd, 3rd stage	$\eta_{s,i}^{nom}$	0.898	–
		4th, 5th, 6th stage		0.868	–
		7th, 8th, 9th, 10th stage		0.830	–
	Low pressure section	1st stage		0.8570	–
		2nd stage		0.8862	–
		3rd stage		0.9118	–
		4th stage		0.9130	–
		5th stage		0.8370	–
		6th stage		0.6529	–
Average specific steam volume for dryness degree = 1	High pressure section	1st stage	$v''_{s,i}$	0.0520	m^3/kg
		2nd stage		0.0599	m^3/kg
		3rd stage		0.0692	m^3/kg
		4th stage		0.0804	m^3/kg
		5th stage		0.0931	m^3/kg
		6th stage		0.1098	m^3/kg
		7th stage		0.1329	m^3/kg
		8th stage		0.1616	m^3/kg
		9th stage		0.1987	m^3/kg
		10th stage		0.2520	m^3/kg
	Low pressure section	3rd stage		1.0950	m^3/kg
		4th stage		1.8190	m^3/kg
		5th stage		3.8100	m^3/kg
		6th stage		17.3500	m^3/kg
Function coefficients	Function $D_{s,i}$		D_D	1000	–
			E_D	2.7473	–
			F_D	1	–
			G_D	7	–
			H_D	1	–
			I_D	0.4786	–
	Function $r_{s,i}$		J_r	1354.7	–
			K_r	2064.72	–
			L_r	1.98	–

(*continued on next page*)

Table A.1 (*continued*)

Parameter name			Symbol	Value	Units
Vapor fraction	Separator		x_{in}	0.8820	–
			x_{out}	0.9999	–
Valve opening degree	Control valve		$\propto_{CV}^{nom\ 0}$	100	%
Inertia gain	Control valve		k_{CV}	0.2	–
Inertia gain	Integral gain constant		k_x	1	s*m
Simplified dynamic model					
Accumulation volume	High pressure section	Dead space	$V_{DS,s}$	4.00	m^3
	Reheater		V_R	470.00	m^3
Specific steam volume, adiabatic exponents	High pressure section	Dead space	$v_{DS,s}$	0.050	m^3/kg
	Reheater		v_R^{avg}	0.250	m^3/kg
	High pressure section	1st stages group	$H_{s,i}$	1.135	–
		2nd stages group		1.130	–
		3rd stages group		1.127	–
	Reheater		H_R^{avg}	1.200	–
	Low pressure section	1st stages group	$H_{s,i}$	1.300	–
		2nd stages group		1.133	–
		3rd stages group		1.130	–
		4th stages group		1.125	–
Mass flow rate	High pressure section	1st stages group	$M_{HP,j}^{nom,out}$	748.638	kg/s
		2nd stages group	$M_{HP,j}^{nom,out}$	668.365	kg/s
		3rd stages group	$M_{HP,j}^{nom,out}$	615.474	kg/s
	Reheater		$M_R^{nom,out}$	504.510	kg/s
	Low pressure section	1st stages group	$M_{LP,j}^{nom,out}$	504.510	kg/s
		2nd stages group	$M_{LP,j}^{nom,out}$	472.772	kg/s
		3rd stages group	$M_{LP,j}^{nom,out}$	449.920	kg/s
		4th stages group	$M_{LP,j}^{nom,out}$	423.810	kg/s
	Separator	Condensate	$M_{MS}^{nom,out}$	111.984	kg/s
Pressure coefficients	Separator	P_{T1}	5.5		
		P_{T2}	4.5		
		P_{T3}	0.12		
		P_{T4}	0.88		
Mass flow rate coefficients	Valve	A_{CV}	1.0398	–	
		B_{CV}	0.99473	–	
Pressure	High pressure section	After valve	$P_{CV}^{nom,\ out}$	4.161	MPa
		1st stages group	$P_{HP,j}^{nom,out}$	4.161	MPa
		2nd stages group	$P_{HP,j}^{nom,out}$	2.729	MPa
		3rd stages group	$P_{HP,j}^{nom,out}$, $P_{HP,n_{LP}}^{nom,out}$	1.673	MPa
	Reheater		$P_R^{nom,out}$	0.6723	MPa
	Low pressure section	1st stages group	$P_{LP,j}^{nom,out}$	0.2344	MPa
		2nd stages group	$P_{LP,j}^{nom,out}$	0.0762	MPa
		3rd stages group		0.0287	MPa
		4th stages group		0.0048	MPa
Temperature	High pressure section				
		1st stages group	$T_{HP,j}^{nom,out}$	525.85	K
		2nd stages group		500.35	K
		3rd stages group	$T_{HP,j}^{nom,out}$	474.55	K
	Low pressure section	1st stages group	$T_{LP,j}^{nom,out}$	397.95	K
		2nd stages group		964.25	K
		3rd stages group		340.45	K
		4th stages group		305.25	K
	Separator		$T_{MS}^{W,nom,out}$	435.65	K
Temperature coefficients	High pressure section	1st stages group	$T_{i,a1}$	0.7710	–
			$T_{i,b1}$	0.0713	–
			$T_{i,c1}$	11.316	–
		2nd stages group	$T_{i,a1}$	0.8107	–
			$T_{i,b1}$	0.0748	–
			$T_{i,c1}$	7.406	–
		3rd stages group	$T_{i,a1}$	0.8547	–
			$T_{i,b1}$	0.0771	–
			$T_{i,c1}$	4.551	–
	Low pressure section	1st stages group	$T_{i,a1}$	0.8389	–
			$T_{i,b1}$	0.0492	–
			$T_{i,c1}$	11.72	–
		2nd stages group	$T_{i,a2}$	0.8139	–
			$T_{i,b2}$	0.1861	–

(*continued on next page*)

Table A.1 (*continued*)

Parameter name			Symbol	Value	Units
		3rd stages group	$T_{i,a2}$	0.8708	–
			$T_{i,b2}$	0.1292	–
		4th stages group	$T_{i,a1}$	0.9290	–
			$T_{i,b1}$	0.0555	–
			$T_{i,c1}$	2.64	–
Power coefficient	High pressure section	1st stages group	$k_{s,i}^{\text{nom}}$	0.112	–
		2nd stages group		0.117	–
		3rd stages group		0.185	–
	Low pressure section		$k_{s,i}^{\text{nom}}$	0.586	–
Enthalpy drop	High pressure section	1st stages group	$\Delta h_{s,i}^{\text{nom,out}}$	71.4	kJ/kg
		2nd stages group		78.5	kJ/kg
		3rd stages group		128.6	kJ/kg
	Low pressure section	1st stages group		172.3	kJ/kg
		2nd stages group		163.4	kJ/kg
		3rd stages group		120.0	kJ/kg
		4th stages group		159.0	kJ/kg
Effective turbine power			η_e^{nom}	471.329	MW

References

[1] I. Dincer, M.A. Rosen, Energy: Energy, Environment and Sustainable Development, Elsevier, 2013 ISBN: 978-0-08-097089-9.
[2] P. Hirsch, K. Duzinkiewicz, M. Grochowski, R. Piotrowski, Two-phase optimizing approach to design assessments of long distance heat transportation for CHP systems, Appl. Energy 182 (2016) 164–176, doi:10.1016/i.apenergy,2016.08.107.
[3] H. Safa, Heat recovery from nuclear power plants, Electr. Power Energy Syst. 42 (2012) 553–559.
[4] J. Dobosz, K. Duzinkiewicz, S. Perycz, W. Próchnicki, Steam Turbine Simulation Model of Transient States for Nuclear Power Unit with WWER-440 Reactor with Omega=Const, Gdańsk University of Technology, Gdansk, 1989 (in Polish).
[5] S. Perycz, W. Próchnicki, Steam Turbine Mathematical Model of Nuclear Power Unit with WWER Reactor, Allowing to Analyze Transient States with Omega=Var, Gdańsk University of Technology, Gdansk, 1989 (in Polish).
[6] W. Grote, Ein Beitrag zur modellbasierten Regelung von Entnahmedampfturbinen, PhD Dissertation, Ruhr-Universität Bochum, Bochum, 2009.
[7] J. Bassas, Development and implementation of a nuclear power plant steam turbine model in the system code ATHLET, Master Thesis, Technische Universität München, München, 2011.
[8] K. Badyda, G. Niewiński, Mathematical steam unit model for energetic unit simulator, chosen issues, Modelowanie inżynierskie 33 (2007) 11–18. Gliwice (in Polish).
[9] A. Chaibakhsh, A. Ghaffari, Steam turbine model, Simul. Modell. Pract. Theory 16 (2008) 1145–1162.
[10] K. Duzinkiewicz, M. Grochowski, A. Kobylarz, K. Kulkowski, Modelling of nuclear power plant steam turbine, Aktualne Problemy Automatyki i Robotyki, Akademicka Oficyna Wydawnicza EXIT, Warszawa, 2014, pp. 603–611.
[11] A. Miller, Mathematical backpressure turbine, Bull. Inst. Heat Eng. 28 (1970) 5–24. Warsaw University of Technology (in Polish).
[12] Z. Jankowski, Ł. Kurpisz, L. Laskowski, J. Łajkowski, A. Miller, J. Portacha, W. Sikora, M. Zgorzelski, Mathematic model of turbine in various conditions e.g. 200 MW power unit, Bull. Inst. Heat Eng. 33 (1972) 1–36. Warsaw University of Technology (in Polish).
[13] J.M. Medina-Flores, M. Picón-Núñez, Modelling the power production of single and multiple extraction steam turbines, Chem. Eng. Sci. 65 (2010) 2811–2820.
[14] G.M. Niewiński, Mathematical model of steam unit, Modelowanie inżynierskie 36 (2008) 365–372 Gliwice (in Polish).
[15] B. Grunwald, J. Lewandowski, A. Miller, J. Plewa, Mathematical steam turbine model for saturated steam, allowing to study dynamics of nuclear power plant unit, Bull. Inst. Heat Eng. 57 (1980) 1–18. Warsaw University of Technology (in Polish).
[16] Ministry of Economy Polish Nuclear Power Programme, Warsaw 2014, http://www.mg.gov.pl/Bezpieczenstwo+gospodarcze/Energetyka+jadrowa/Program+polskiej+energetyki+jadrowej (accessed 01.28.14).
[17] W. Bolek, J. Sasiadek, T. Wisniewski, Two-valve control of large steam turbine, Control Eng. Pract. 10 (2002) 365–377.
[18] D. Zivković, Nonlinear mathematical model of the condensing steam turbine, Facta Univ. Mech. Eng. 1 (7) (2000) 871–878.
[19] M. Klawe, D. Pietrzak, Developing Usable Version Dyne and DROP Programs and their Documentation and Manuals, The Institute of Energy, Institute of Heat Engineering, Warszawa, 1982 (in Polish).
[20] K. Duzinkiewicz, M. Grochowski, K. Kobylarz, K. Kulkowski, Dynamic model of nuclear power plant steam turbine, Arch. Control Sci. 25 (1) (2015) 65–86 (LXI).
[21] K. Duzinkiewicz, T.K. Nowak, R. Piotrowski, Fractional neutron point kinetics equations for nuclear reactor dynamics – numerical solution investigations, Ann. Nuclear Energy 73 (2014) 317–329.
[22] K. Duzinkiewicz, T.K. Nowak, R. Piotrowski, Numerical solution analysis of fractional point kinetics and heat exchange in nuclear reactor, Nuclear Eng. Des. 281 (2015) 121–130.
[23] K. Duzinkiewicz, M. Grochowski, K. Kulkowski, Efficiency of process abnormality detection in steam turbine of nuclear power plant using multivariate statistical analysis methods, in: Zeszyty Naukowe Wydziału Elektrotechniki i Automatyki Politechniki Gdańskiej, 2015, pp. 107–110.